

<https://doi.org/10.1038/s44328-025-00065-8>

Molecularly imprinted polymer-based electrochemical sensors for amino acid detection: towards wearable sensing

**Ruotong Gao** **Muhammad Khatib** & **Zhenan Bao**

Continuous, non-invasive monitoring of physiological health is a significant objective in modern medicine and personalized wellness. To efficiently capture physiological data and diagnostic metrics, the ideal biofluid/medium for health monitoring should be non-invasive, easy to access, and contains a variety of physiologically significant analytes. Sweat is a particularly promising biofluid for real-time monitoring due to its ease of usage and rich milieu of metabolic and potentially diagnostic biomarkers. Within sweat, amino acids are of particular diagnostic interest due to their direct correlation with a spectrum of metabolic disorders, chronic illnesses, and overall health. Molecularly Imprinted Polymers (MIPs) have emerged as a promising class of synthetic, antibody-mimetic receptors that offer a robust, stable, and cost-effective alternative to traditional biological recognition elements. This review provides a comprehensive examination of MIP-based sensors for the detection of amino acids in sweat. It commences with an overview of the current literature around wearable sensing and real-time health monitoring. Then it presents a dissection of sweat composition and its utility as a diagnostic fluid with a following exploration of the role of amino acids as pivotal biomarkers in sweat. The review then discusses the fundamental principles of molecular imprinting, detailing various synthesis methodologies and the underlying physicochemical binding mechanisms governing MIP-analyte interactions. Subsequently, the specifics of MIP-based sensor construction for sweat analysis are investigated such as substrate selection, various signal transduction modalities with an emphasis on electrochemical techniques, nanomaterial integration, and current methods for sweat induction in wearables. This review concludes with analyzing current research trajectories, addressing the scientific and technical challenges such as sensor regeneration, physiological differences in amino acid concentrations, and explores the opportunities for future applications like point-of-care diagnostics, management of chronic diseases, and integration with artificial intelligence for personalized health analytics and health monitoring.

Continuous health condition monitoring and proactive intervention (ideally before the onset of disease) are essential developments for improving healthcare^{1–8}. The status quo focuses primarily on reactive medical intervention, meaning patients typically seek care after developing noticeable symptoms. Many chronic and geriatric diseases also require significant monitoring, currently performed through a variety of invasive procedures, for disease prognosis and overall health. This highlights the urgent need to develop devices that provide continuous, real-time insights for health monitoring. In recent years, sweat/wearable biosensors have emerged as a promising direction for diagnostic and prognostic care^{1,3,4,7}. There have been

numerous developments in wearable devices for accurate measurement of biophysical parameters, such as blood pressure, galvanic skin response (GSR), heart rate, and body temperature, though recent studies have drawn more attention onto monitoring direct information on the physiological and metabolic biomarkers of the human body^{1,9,10}. This movement towards wearable biomarker detection and diagnosis is not limited to sweat; however, Heikenfeld and colleagues comprehensively reviewed biochemical monitoring across various biofluids⁵. For sweat sensors, these recent advances demonstrate a progression of biosensing to combine component innovations, such as novel receptors or microfluidic designs, to the

construction of fully integrated systems^{11–13}. By combining sensor arrays, flexible electronics, and biochemical receptors, with recent studies on data science and machine learning algorithms developing to interpret biosensor data, the infrastructure for wearable biosensors has improved significantly^{14,15}. As illustrated in Fig. 1, from the specifics of MIP synthesis, sensor fabrication strategies, and various electrochemical sensing modalities to sweat induction and biomarker detection, this review systematically examines the core components and provides a comprehensive overview of MIP-based AA sweat sensing. This structure provides a comprehensive framework for understanding the current landscape, future trajectory of the field, and applicability to health monitoring.

Among the various biofluids available for analysis, sweat has emerged as a particularly compelling sample for wearable sensing. Gao and coworkers' review on wearable sweat sensors offers a comprehensive and broader perspective on the area of sweat sensing¹⁶. The conventional gold standard biofluid, blood (and its constituents), is information-rich; however, access is invasive¹⁷. In contrast, other biofluids, such as, saliva and urine, have limitations for continuous monitoring, including sampling difficulty,

contamination and inconsistency¹. On the other hand, sweat is readily and non-invasively available, consistently detectable, and contains a vast secretome of biomarkers reflecting metabolic state, diseases, and overall health^{1,7,9,11,17}.

Since the initial proposals for real-time sweat analysis, much research has been directed to the monitoring of various analytes, such as electrolytes, metabolites, proteins, and trace elements¹. However, within the varied composition of sweat, amino acids stand out as significant molecular targets for analysis. Amino acids play a crucial role in human metabolic function due to their utilization of carbon skeletons in energy production and glucose conversion, while also serving as essential precursors for other vital biomolecules, including the nucleotides of DNA and RNA, as well as the heme group in hemoglobin. However, recent discoveries have further established amino acids as sophisticated signaling molecules that play an active role in regulating cellular and bodily physiology, which in turn acts as potential biomarkers for many diseases^{18,19}. Current literature demonstrates that glutamate and glycine act as the primary excitatory and inhibitory neurotransmitters in the central

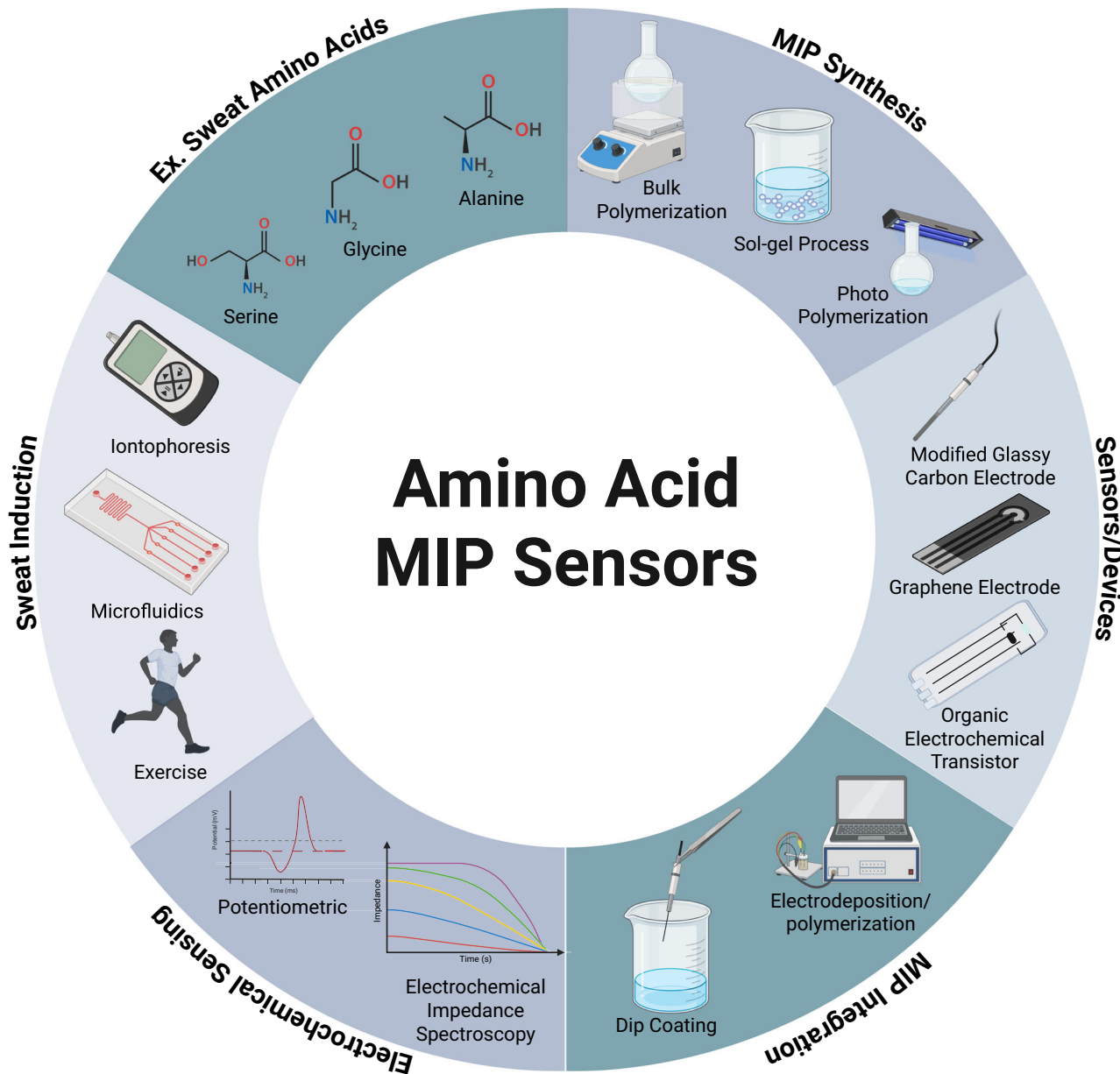


Fig. 1 | Graphical illustration of the key components and potential applications of MIP-Based Amino Acid (AA) Sensors, from sweat induction and biomarkers to MIP synthesis, sensor fabrication, and electrochemical sensing methods discussed in this review.

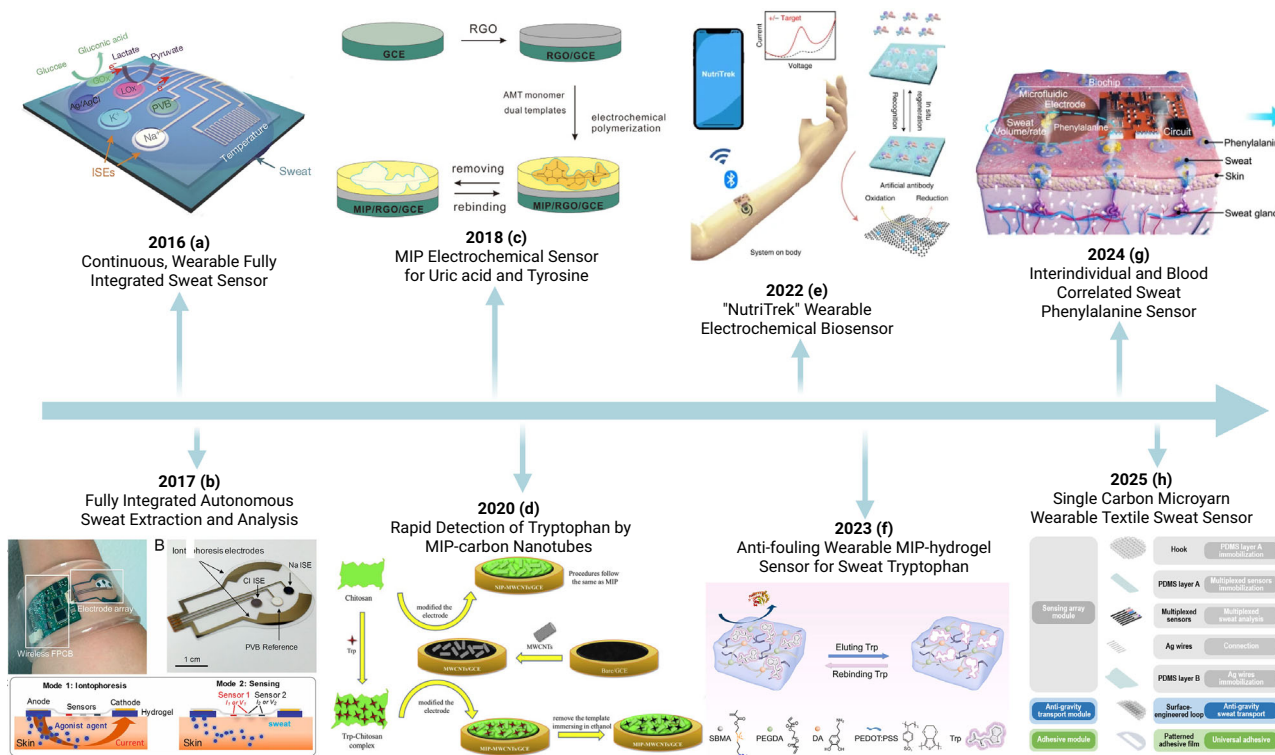


Fig. 2 | A timeline of key milestones in the development of general wearable sweat sensors from 2016 to 2025. The figure highlights the technological progression of MIP sensors from a fully integrated multiplexed sensing platforms combined with on-demand sweat induction¹⁴², b refinement of selective recognition layers, such as the use of creation of a fully integrated sweat analysis platform¹⁴³, c development of MIP electrochemical sensors for Tyrosine and Uric Acid¹⁴⁴, d integration of CNTs

and nanomaterials in a MIP sensor for Tryptophan detection¹⁴⁵, e Comprehensive wearable MIP biosensors for personalized nutrition⁹, f anti-fouling wearable MIP sensing for sweat tryptophan¹³³, g point-of-care diagnostics validated against blood standards for metabolic disorders like phenylketonuria¹⁴⁶, h to recent studies working towards textile-integrated sensors¹⁴⁷.

nervous system, respectively²⁰. Others, like tryptophan and tyrosine, are essential precursors for key neurotransmitters, such as serotonin and dopamine, directly linking diet to mood and cognitive function²⁰. Furthermore, amino acids, such as arginine, glutamine, and tryptophan are now recognized as critical modulators of the immune system, directing immune cell activation, cardiovascular system/disorders, and influencing the gut-brain axis¹⁹. This evolving understanding demonstrates that amino acids are not simply static indicators of nutritional status but as significant biomarkers for the real-time state of the body's metabolic, nervous, and immune systems, which positions them as valuable targets for continuous health monitoring^{18–20}. The practical realization of quantifying amino acids in sweat requires the construction of robust and highly selective recognition elements. While natural receptors like antibodies and enzymes have been historically prevalent for biosensing, their application in wearable technology is significantly limited by high production costs, complex purification, selectivity, and stability²¹. A synthetic alternative, Molecularly Imprinted Polymers (MIPs) have recently emerged as a promising and disruptive alternative^{22,23}. These antibody-mimetic materials are engineered with tailored recognition cavities that are sterically and chemically complementary to specific target molecules. MIPs offer high sensitivity and selectivity with high physical durability, resistance to chemical and thermal degradation, and low-cost production. Figure 2 demonstrates a timeline of general sweat sensors and their evolution towards MIP-based AA-specific wearable sensors. This progression highlights the various milestones of the technology from foundational research on wearable sweat sensors and integrated platforms towards highly sensitive, wearable monitoring of specific metabolic biomarkers and amino acids, overall providing a comprehensive overview of the many years of significant research preceding MIP-based AA sensors.

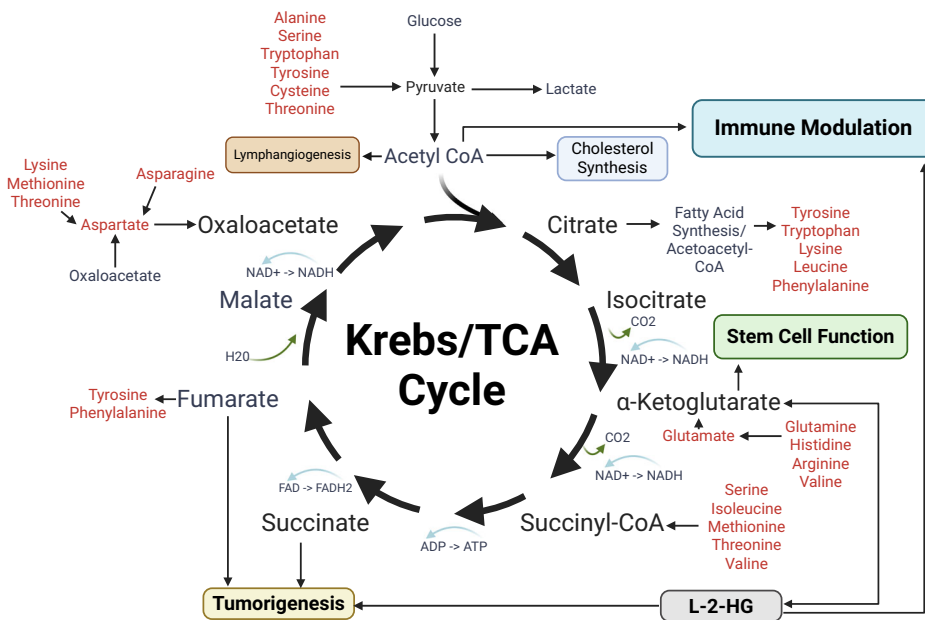
This review provides a comprehensive overview of the current state of MIP-based, wearable sensors for amino acid detection in sweat. It begins by detailing the physiological importance of sweat as a diagnostic medium and the clinical significance of its amino acid constituents. Subsequently, the review explores the fundamental principles of molecular imprinting and the engineering considerations for sensor design, including substrate selection and signal transduction. It then evaluates the current literature/status quo, addressing key challenges which may impede clinical translation, and outlines future opportunities for this technology to advance health monitoring.

Sweat physiology and biomarkers

The diagnostic potential and composition of sweat

Sweat is a complex biofluid secreted by glands within the skin. It primarily serves the physiological function of thermoregulation, moisturization, immune defense, and electrolyte and pH balance¹²⁴. Sweat is produced by two distinct types of glands: eccrine and apocrine, both of which have been explored for their potential diagnostic capabilities. Apocrine glands are located at specific anatomical regions, such as the axilla and secrete a viscous, lipid-rich fluid into hair follicles^{24,25}. This distribution thus makes it less favorable for diagnostic purposes, with eccrine sweat garnering more significant scientific attention, as eccrine glands are distributed across the entire body surface and secrete a clear, aqueous fluid that is a more direct reflection of the constituents of blood plasma^{25–27}. Generation of this sweat can be induced through thermoregulation during physical activity or, for on-demand analysis in sedentary individuals, through localized iontophoretic delivery of cholinergic agonists or electrical stimulation. The diagnostic value of eccrine sweat lies in its rich and dynamic chemical composition. While predominantly composed of water and electrolytes, such as sodium,

Fig. 3 | Illustration of the Krebs/TCA (tricarboxylic acid) cycle, its metabolism, and how it acts as a central hub of cellular metabolism, illustrating the entry points, roles, and connections of various amino acids (red font). Prepared based on summary by Martinez-Reyes et al.³⁰.



potassium (K^+), and chloride (Cl^-), sweat contains a diverse array of organic and inorganic molecules that provide a multiparametric window into an individual's physiological state¹. This secretome includes a variety of metabolites, including lactate from anaerobic glycolysis and urea from the hepatic urea cycle; hormones like cortisol, which is a key indicator of physiological stress; exogenous agents, including therapeutic drugs and their metabolites; and, critically for this review, a wide spectrum of amino acids^{1,25,26,28}.

Amino acids and diseases

Amino acids are commonly recognized as the fundamental building blocks of proteins. However, their physiological roles extend far beyond proteogenesis, including crucial biological mechanisms like neurotransmission, hormone synthesis, and cellular energy metabolism^{28,29}. Tight bodily regulation on amino acid concentrations in biofluids consequently posits the dysregulation of amino acid metabolism as a hallmark of numerous health conditions. As depicted in Fig. 3, the Krebs/TCA cycle acts as a central hub connecting amino acid catabolism with cellular energy production, with the central role of these amino acids in critical metabolic pathways highlighting why monitoring their concentrations is beneficial for the early detection and management of many associated pathological conditions³⁰. Many amino acids can be converted into key metabolic intermediates within the cycle, contributing to the cell's energy supply, serving as precursors for biosynthesis, tumorigenesis, stem cell function, and physiological function, demonstrating how defects in amino acid processing can ultimately lead to pathological conditions (Table 1)³⁰. Genetic metabolic disorders provide the clearest examples of amino acid dysfunction-related conditions, such as in Phenylketonuria (PKU), a deficiency in phenylalanine hydroxylase that causes toxic accumulation of phenylalanine. This has been found to lead to neurological damage by competitively inhibiting the transport of other crucial amino acids, such as tyrosine and tryptophan, across the blood-brain barrier. According to van Spronsen and coworkers, management of PKU aims to maintain plasma phenylalanine concentrations between 120 and 600 $\mu\text{mol/L}$ in adolescents and adults to prevent this toxicity³¹. Similarly, Maple Syrup Urine Disease (MSUD), a disease that results from a defective branched-chain α -ketoacid dehydrogenase (BCKDH) complex, can be significantly ameliorated with early diagnosis. Recent studies have found that diagnosis and dietary intervention within the first 5–7 days of life are critical for preventing severe neurological complications³². The disease causes a buildup of branched-chain amino acids (BCAAs), which are

primarily driven by excess leucine, resulting in neurotoxicity, saturated brain transporters and impaired neurotransmitter synthesis³². Beyond monogenic diseases, chronic conditions also feature various amino acid imbalances. In advanced liver cirrhosis, for instance, impaired hepatic function leads to elevated aromatic amino acids (AAAs) and depleted BCAAs. According to Meyer and coworkers, the resulting low Fischer Ratio (the molar ratio of BCAA to AAA), particularly a value below 1.0, is a key factor that contributes to hepatic encephalopathy and muscle atrophy³³. Furthermore, altered amino acid metabolism, particularly for BCAAs, have been found to be particularly implicated in cardiovascular diseases. Elevated levels of BCAAs have been found to be associated with an increased risk of atherosclerosis and heart failure. Mansoori and coworkers note that some heart failure patients exhibit a 2-fold increase in plasma BCAA levels, while impaired BCAA catabolism in the heart contributes to contractile dysfunction³⁴. Another important amino acid implicated in cardiovascular disease, arginine, as the precursor to nitric oxide (NO), stands as a key molecule for vasodilation and maintaining vascular health. Recent studies have found increasing evidence of its role and connection to hypertension and atherosclerosis, with Oyovwi and coworkers demonstrating the bioavailability of L-arginine for endothelial NO synthase (eNOS) and its essentiality for preventing endothelial dysfunction³⁵. Additionally, high levels of homocysteine, a metabolite of methionine, are recognized as an independent biomarker for cardiovascular disease. Jakubowski and Witucki specified that homocysteine levels exceeding 15 $\mu\text{mol/L}$ are associated with increased risk, promoting endothelial damage, inflammation, and oxidative stress³⁶. Amino acid metabolism is also actively reprogrammed in complex diseases like cancer and is increasingly implicated in neuropsychiatric disorders. According to Lieu et al., cancer metabolism is dependent on amino acids and their pathways, such as the central carbon metabolism, including glycolysis and the tricarboxylic acid cycle²⁸. Furthermore, cancers exhibit a heightened dependency on specific amino acids to fuel proliferation, such as glutamine to replenish the TCA cycle and synthesize nucleotides, and an over-reliance on the serine-glycine pathway for DNA replication precursors²⁸. Tumors also manipulate arginine and tryptophan metabolism within their microenvironment to evade the immune system. Recent studies have found that many tumors accomplish this by depleting arginine to starve T-cells, often due to the silencing of the argininosuccinate synthetase 1 (ASS1) gene and upregulating the IDO enzyme to convert tryptophan into immunosuppressive kynurene metabolites^{28,37}. Overall, amino acid metabolism has been shown to play a critical role in cancer metabolism,

Table 1 | Key Amino Acid Biomarkers in Sweat, Their Properties, and Associated Health Conditions

Amino Acid	Polarity	Side Group	Essentiality	Health Condition(s)	Sweat Conc. (μM)	References
Tyrosine	Polar, Amphiphatic	Phenol group	Conditionally Essential	Tyrosinemia, Non-Alcoholic Liver Disease, Neuropsychiatric disorders, Alkaptonuria, Depression	112 ± 23	43–47
Leucine	Non-polar, Hydrophobic	Isobutyl group (Branched chain)	Essential	Type 2 Diabetes, Diabetic Retinopathy, Sarcopenic Risk	112 ± 7.2	48–50
Glycine	Non-polar (often considered neutral)	Hydrogen atom	Conditionally, Non-Essential	Cardiovascular Disease, Type 2 Diabetes, Cognitive Decline	1024 ± 122	51–54
Phenylalanine	Non-polar, Hydrophobic	Benzyl group (Aromatic)	Essential	Phenylketonuria (PKU), Parkinson's Disease, Heart Failure, Alkaptonuria, Radiographic Knee Osteoarthritis	203 ± 14.4	45,55–57
Arginine	Positively Charged, Polar, Basic	Guanidinium group	Conditionally Essential	Cardiovascular Disease (Hypertension, atherosclerosis, HF, CAD), Depression	13.8 ± 9.5	58–62
Citrulline	Polar, Neutral	Ureido group	Non-Essential	Cardiovascular Disease, Type 2 Diabetes, Depression	8.2 ± 5.2	61–64
Serine	Polar, Uncharged	Hydroxymethyl group	Conditionally, Non-Essential	Alzheimer's Disease, Kidney Disease, Cancer	1664 ± 128	53,54,65–67
Alanine	Non-polar, Hydrophobic	Methyl group	Non-Essential	Type 2 Diabetes, Sarcopenia, Gestational Diabetes Mellitus	458 ± 8.0	51,68,69
Ornithine	Positively Charged, Polar, Basic	3-aminopropyl group	Non-proteinogenic, Conditionally, Essential	Depression, Parkinson's, Bladder Cancer, Cardiovascular Disease (Through GABR)	302.76 ± 139.41	55,61,70–72
Tryptophan	Non-polar, Hydrophobic	Indole group (Aromatic)	Essential	Cancer, Neurodegenerative Disease	43.27 ± 20.25	38–40,73,74,138

GABR Global Arginine Bioavailability Ratio.

positing amino acid monitoring to be a promising target for understanding tumor progression and diagnosis.

In neurological disorders, imbalances in tryptophan metabolism have been demonstrated to contribute to the biology of depression through tryptophan's sole precursor relationship to the mood-regulating neurotransmitter serotonin³⁸. During inflammation or stress, tryptophan is shunted away from serotonin synthesis and down the kynurenine pathway. According to Correia and Vale, this diversion is significant, with up to 95% of tryptophan being metabolized via the kynurenine pathway under inflammatory conditions³⁸. This tryptophan steal mechanism further contributes to depressive symptoms through both serotonin depletion and the production of neurotoxic metabolites^{38,39}. Gong et al. specified that pro-inflammatory cytokines directly activate enzymes, such as IDO1, which initiates this steal³⁹. This link is further reinforced by findings that analyze acute tryptophan deletion, both experimentally and naturally, triggered a rapid relapse in depression and anxiety in patients undergoing serotonergic antidepressants^{40,41}. Recent studies have also found this to be relevant in dementia, with Aquilani et al. reporting a 20–30% reduction in the plasma ratio of tryptophan to other competing amino acids in Alzheimer's patients, suggesting impaired brain availability⁴². Furthermore, as certain amino acids are direct metabolic precursors to key neurotransmitters, for instance, tryptophan is the precursor to serotonin, and tyrosine is the precursor to dopamine, amino acids promise future neurological insights. Although all of its mechanisms are not yet fully understood, the ability to non-invasively track these neurochemical precursors in sweat could provide specific, biologically significant data to complement psychiatric diagnostics and monitor therapeutic responses. The following table summarizes ten key amino acids that serve as potential biomarkers in sweat, detailing their essential properties and typical concentrations alongside the specific health conditions the dysregulation indicates^{43–74}.

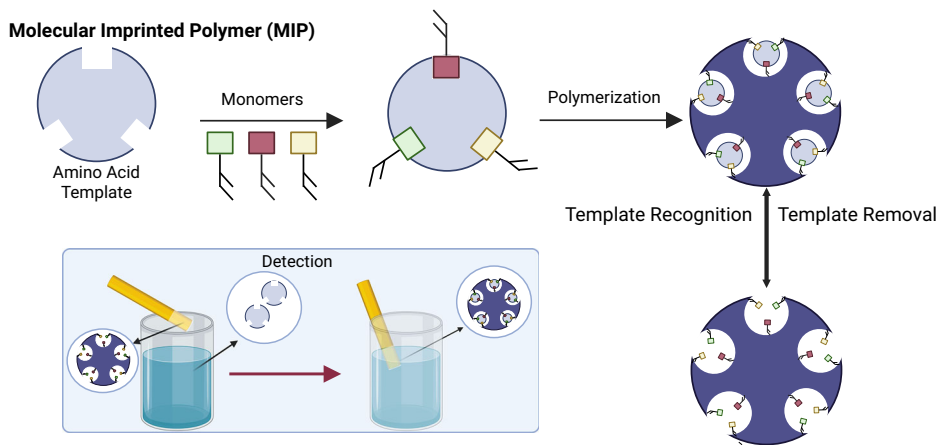
MIPs synthesis

MIPs are highly cross-linked synthetic polymers that may act similarly to natural antibodies⁷⁵. Functionally, they are engineered to possess tailored recognition sites complementary to a specific target molecule, mimicking biological receptors. Its polymerization and crosslinking result in a rigid, three-dimensional polymer network that effectively frames the functional monomers in an optimized spatial arrangement around the template, creating a molecularly shaped cavity that is capable of selectively rebinding the target analyte in a lock and key fashion⁷⁶. This process is illustrated in Fig. 4, demonstrating a schematic overview of the MIP synthesis process and providing a rudimentary understanding of how it can selectively rebind and be used in a sensor setting. Due to their highly crosslinked nature, MIPs can be optimized to have stability in sensing, with some capable of withstanding harsh environmental conditions, including high temperatures (up to 300 °C in some cases), extreme pH, exposure to organic solvents, and long shelf life, all without loss of function^{77,78}. By contrast, biological receptors can be fragile, with antibodies and enzymes being susceptible to irreversible denaturation from shifts in temperature or pH. MIPs also offer substantial advantages in terms of cost and production. The synthesis process for MIPs is relatively straightforward and significantly less expensive and time-consuming than the production of biological receptors. For example, the generation of high-affinity monoclonal antibodies is typically complex and costly, involving animal immunization, cell line development, and extensive purification⁷⁹. Similarly, producing enzymes often requires laborious microbial screening, cloning, and large-scale fermentation⁸⁰. Although the highest-affinity antibodies may still outperform MIPs, numerous studies have demonstrated that MIPs can achieve sensitivity and selectivity that are comparable or even superior to their biological counterparts^{81,82}. The synthesis of these MIPs can be conducted using various methods and different compounds chosen for specific usages (Table 2).

Bulk free-radical polymerization (FRP)

The most established and widely practiced family of techniques for MIP synthesis is free-radical polymerization (FRP), which includes bulk,

Fig. 4 | Schematic diagram of the molecular imprinting process. An amino acid template molecule directs the assembly of functional monomers. After polymerization, the template is removed, leaving a complementary binding cavity. The MIP can then selectively rebind the target analyte for detection.



precipitation, and emulsion polymerization (all of which have been successfully applied to amino acid MIP syntheses). Bulk polymerization is currently the most widely used method for MIP synthesis due to its simplicity and versatility⁸³. The procedure involves mixing the template, functional monomer, cross-linker, and initiator in a porogenic solvent. Upon initiating polymerization (typically thermally in bulk polymerization), a crosslinked MIP polymer network is formed⁸⁴. While the synthesis is straightforward, the aggressive post-processing by grinding remains a drawback as it can potentially produce irregularly shaped particles with a larger size distribution or damage some of the pre-formed recognition cavities. Despite these limitations, bulk polymerization is still a viable method for MIPs, such as amino acid MIP syntheses for L-Lysine by Pisarev and Polyakova⁸⁵. Rather than using traditional thermal initiation, FRP can additionally be initiated with methods, such as ultraviolet (UV) light or electron beams. Photopolymerization, however, allows for enhanced spatial and temporal control over the reaction and can preserve the integrity of thermally sensitive templates and pre-polymerization complexes⁸⁶. This approach and its advantages can be seen in the works of Chen et al. for L-Histidine⁸⁷ and Najafizadeh et al. for L-Phenylalanine⁸⁸. Furthermore, Miao et al.⁸⁹ employed a more novel technique of electron beam irradiation to polymerize an MAA-based MIP for the adsorption and recognition of L-Tyrosine. These radiation-based methods may offer different reaction kinetics and potentially lead to materials with unique network structures, though their usage has not been fully explored in the current literature.

Precipitation and emulsion polymerization

To address the disadvantages of bulk polymerization, i.e., the destructive grinding step and resulting particle irregularity, both precipitation and emulsion polymerization methods were designed to produce uniform, spherical micro or nanoparticles directly in a solution. Precipitation polymerization is particularly notable for producing high yields of surfactant-free particles. In precipitation polymerization, all components are dissolved in a larger volume of porogen. As polymerization proceeds, the growing polymer chains become insoluble in the solvent and precipitate out as discrete, monodisperse spherical particles⁹⁰. On the other hand, emulsion polymerization techniques, such as the mini-emulsion approach used for L-Proline by Mustafa et al.⁹¹ and the copolymerization used for L-Tryptophan by Xia et al.⁹², employed surfactants to stabilize monomer droplets in an immiscible continuous phase to form polymer latex particles. This residual surfactant in emulsion polymerization necessitates further post-processing and washing, making the procedure unideal for creating undisturbed recognition cavities (Table 2).

The sol-gel process

Compared to emulsion polymerization, the sol-gel process is drastically different, offering a distinct procedure involving the hydrolysis and polycondensation of metal alkoxide precursors, such as silicon alkoxides like

tetraethyl orthosilicate (TEOS) or functionalized silanes, to form a rigid, highly porous, and stable inorganic network⁹³. A functionalized precursor, such as 3-aminopropyltriethoxysilane (APTES) is often used, which acts as both a network forming agent and a functional monomer. This methodology was strategically employed for the synthesis of MIPs targeting the small, non-polar amino acids L-Alanine⁹⁴ and L-Valine⁹⁵. In the work by Aryan et al.⁹⁴, the sol-gel process was used to create L-Alanine-imprinted polymers on the surface of silica nanoparticles (SiO₂ NPs), which were then used to modify an electrode for electrochemical sensing. Thus, the sol-gel process is ideally suited for surface imprinting and offers significant kinetic advantages over traditional bulk imprinting. By confining the recognition sites to the material/electrode's surface, issues of poor site accessibility and slow mass transfer are effectively eliminated⁹⁶. The use of high-surface-area nanoparticles as a support further amplifies the analytical signal for electrochemical sensors. The sol-gel process, as employed in the L-Alanine sensor⁹⁴, combines the physical robustness of a silica matrix with the kinetic and accessibility benefits of surface-imprinted nanoparticles. The combined theoretical and experimental approach taken by Azalina et al.⁹⁵ for L-Valine demonstrates the high degree of control and sensitivity with this method (Table 2).

Electrochemical polymerization

Electrochemical polymerization is a prominent surface-imprinting technique involving the *in situ* growth of a polymer film directly onto the surface of an electrode by applying an electrical potential. Its primary advantage lies within its one-step fabrication of a thin, uniform, and strongly adhered MIP film integrated with the signal transducer⁹⁷. This approach eliminates the need for multi-step procedures for immobilizing pre-synthesized MIP particles onto a sensor surface. The work of Yu et al.⁹⁸ in developing a sensor for L-Glutamic Acid utilizes electrochemical polymerization to deposit a film of 4,6-diaminoresorcinol in the presence of the L-Glutamic Acid template. Crucially, this was not done on a bare electrode but pre-modified with carbon nanotubes (CNTs). By first modifying the electrode with CNTs, a nanostructured scaffold is created that dramatically enhances the electroactive surface area available with the subsequent electropolymerization for the selective MIP layer. This combination, the modified electrode's amplified signal transduction with the MIP providing specific molecular recognition, acts as the key for the sensitive determination of L-Glutamic Acid in pig serum⁹⁸.

Trends in MIP Synthesis

A common trend in MIP polymerization, Methacrylic Acid (MAA) has been widely used as a functional monomer (L-Cysteine⁹⁹, L-Histidine⁸⁷, L-Phenylalanine⁸⁸, L-Tyrosine⁸⁹, and L-Lysine^{85,100}). This commonality is a rational design choice for non-covalent imprinting. Amino acids are zwitterionic molecules, possessing both a protonated amine group and a deprotonated carboxyl group at physiological pH, making them

Table 2. | Summary of Examples of Reported (selected to cover a wide variety of synthesis methods) MIPs for Various Amino Acids

Amino Acid	Method of Synthesis	Reagents (Monomer; Crosslinker)	Usage	Refs.
L-Asparagine	Free-Radical Polymerization	AAm & HEMA; EDMA	Recognition and removal in food	139
L-Alanine	Sol-Gel Process	APTES; TEOS	Determination in urine samples	94
L-Cysteine	Free-Radical Polymerization	Methacrylic acid, NIPAM, & Aam; MBAA	Electrochemical enantioanalysis	99
L-Glutamic Acid	Electrochemical Polymerization	4,6-diaminoresorcinol (self-crosslinked)	Determination in pig serum	98
L-Histidine	Photo Polymerization	Methacrylic Acid; EDMA	Optical detection	87
L-Leucine	Mechanochemical Polymerization	AAm; MBAA	Affinity biopurification	140
L-Lysine	Bulk Polymerization	Methacrylic Acid; EDMA	Recognition	85
L-Phenylalanine	UV Polymerization	Methacrylic Acid; EDMA	Reduction of concentration in serum	88
L-Proline	Mini-emulsion polymerization	Vinyl Imidazole; EDMA	Diagnosis of metabolic disorders	91
L-Tyrosine	Electron beam irradiation	Methacrylic Acid; EDMA	Adsorption and recognition	89
L-Tryptophan	Emulsion copolymerization	4-vinylbenzoic acid; EDMA	Electrochemical sensor for detection	92
L-Valine	Sol-gel Process	APTES; TEOS	Identification and selection of Valine	95

AAm Acrylamide, APTES (3-Aminopropyl)triethoxysilane, EDMA Ethylene glycol dimethacrylate, HEMA Hydroxyethyl methacrylate, MBAA N,N'-Methylenebis(acrylamide), NIPAM N-Isopropylacrylamide, TEOS Tetraethyl orthosilicate, UV Ultraviolet.

excellent at forming multiple hydrogen bonds¹⁰¹. For a high-fidelity MIP to be formed, the prepolymerization complex between the template and the functional monomer must be strong and stable. The carboxylic acid moiety of MAA is a superb hydrogen bond donor and acceptor, allowing it to form stable, often dimeric, hydrogen-bonded complexes with the functional groups on the amino acid template, further ensuring that the spatial arrangement of the monomer around the template is maintained throughout the polymerization process. While MAA is a powerful general-purpose monomer, its interactions may not be optimal for all templates. For instance, Mustafa et al. selected Vinyl Imidazole as the functional monomer for imprinting L-Proline, as its α -amino group is a secondary amine incorporated into a rigid five-membered pyrrolidine ring⁹¹. This structure sterically hinders interactions that are favorable for primary amines, leading to the use of the imidazole ring of the monomer, with its aromatic character and basic nitrogen atoms, to offer more favorable steric complementarity and electronic interactions (e.g., hydrogen bonding and $\pi - \pi$ stacking) with the proline ring. Similarly, for the imprinting of L-Tryptophan, which possesses a large, hydrophobic indole side chain, Xia et al.⁹² employed 4-vinylbenzoic acid as this monomer contains both a carboxylic acid group for hydrogen bonding with the amino acid backbone and a benzene ring strategically included to induce $\pi - \pi$ stacking interactions with the L-Tryptophan's indole ring. These examples both demonstrate the necessity of specific monomers to engage in interactions with both the conserved backbone and the unique side chain of the target amino acid.

Sensor transduction and fabrication

Sensor transduction

A sensor's transduction mechanism is the critical component that converts a molecular recognition event, in this context, an amino acid binding to an MIP, into a measurable analytical signal. While several transduction strategies exist, including optical and mass-based methods, electrochemical techniques are typically used for MIP-based sensors due to their high sensitivity, wide range of detection, ease of construction, and potential for miniaturization and flexibility for portable devices^{19,22}. This section provides an overview of the most common electrochemical transduction methods used for detecting amino acids. Table 3 summarizes the performance characteristics of several recently reported electrochemical MIP sensors targeting a range of amino acids. As shown in the table, these sensors employ a variety of electrode modifications and detection techniques to achieve impressive limits of detection (LOD) and wide linear ranges, highlighting

the versatility and power of this approach. The following subsections will delve into the principles of these key electrochemical techniques.

Electrochemical impedance spectroscopy

Electrochemical Impedance Spectroscopy (EIS) is a label-free, non-faradaic method that probes the electrical properties of the electrode-electrolyte interface by applying a small AC potential over a range of frequencies. EIS is typically performed using a three-electrode setup, as seen in Fig. 5a, and can easily detect surface interactions and allows the MIP layer to perform with very high precision and label-less detection of analytes at extremely low concentrations¹⁰². Alam et al.'s work on Tryptophan detection demonstrates the usage of EIS in amino acid MIP sensing with extremely high sensitivity, with a linear range of 10 pM - 80 μ M, a LOD of 8 pM, and high selectivity for Tryptophan detection¹⁰³. Similarly, Roy et al.'s detection of Tyrosine through a modified-ITO sensor using EIS demonstrates an extremely low LOD (6.63 pM (EIS)) and highly significant linear range (100 fM-1 mM)¹⁰⁴. Though not an amino acid, dopamine was successfully monitored with high sensitivity by Hemed et al. through an MIP EIS-based sensor with a large linear range of 1 nM to 10 mM, a LOD of 0.76 nM, and selectivity¹⁰⁵. Furthermore, Hemed et al. demonstrate sensing in PC-12 cell cultures, confirming its ability to sense in biological media, and, importantly, demonstrate near-complete reversibility by applying a small voltage pulse¹⁰⁵. Though less fully explored than many other techniques for amino acid MIP usages, EIS has demonstrated substantial potential for biosensing with high biocompatibility, precise measurements, and a large range of detection.

Voltammetric techniques

Pulse-based voltammetric techniques, specifically Differential Pulse Voltammetry (DPV) and Square Wave Voltammetry (SWV), have been widely used for amino acid MIP sensors. These pulse techniques (setup shown in Fig. 5b) are specifically designed to discriminate between Faradaic current and non-Faradaic charging current, which allows the sensors to achieve the low LODs required for the analysis of trace-level biomarkers¹⁰⁸. However, the standard method of Cyclic Voltammetry (CV) is still commonly used, with studies from Zhang, and Li, and Dinu, and Apetrei, demonstrating a low limit of detection with a large linear range^{106,107}.

Differential Pulse Voltammetry (DPV)

DPV is frequently employed within recent literature, utilized in the detection of L-Alanine⁹⁴, L-Cysteine⁹⁹, L-Glutamic Acid⁹⁸, L-Phenylalanine¹⁰⁹, and L-Tryptophan⁹². This popularity stems from its well-suited nature for quantitative analysis in complex media. By sampling the current late in the

Table 3 | Performance Characteristics of Some Reported (selected based of diversity of electrochemical detection methods and demonstration of a wide performance spectrum) Electrochemical MIP Sensors for Amino Acid Detection

Amino Acid	Electrode Modification	Detection Method	LOD	Linear Range	Refs.
L-Alanine	CPE	DPV	0.6 μ M	1.0–150.0 μ M	94
L-Aspartic-Acid	PGE	SWV	~1.11 ng/mL	0.005–1.0 μ g/mL	110
L-Cysteine	Magnetic GCE	DPV	~0.74 pg/mL	~1–12 pg/mL	99
L-Glutamic Acid	MWCNT/GCE	DPV	5.13 nM	0.01–100 μ M	98
L-Histidine	OECT-based	OECT	100 nM	100nM–10 μ M	113
L-Phenylalanine	f-MWCNT/GCE	DPV	6.83 nM	0.01–100 μ M	109
L-Sarcosine	AuNP/SPCE	EIS	0.84 ng/mL	1–1600 ng/mL	141
L-Serine	PGE	SWV	~0.24 nM	0.001–0.1 μ M	111
L-Tryptophan	Chem-MWCNT/GCE	DPV	6 nM	0.01–100 μ M	92
L-Tryptophan	PPy(FeCN)/SPCE	CV	105 nM	0.33–10.5 μ M	107
L-Tryptophan	Lysozyme Amyloid Fibril	EIS	8pM	10 pM–80 μ M	103
L-Tyrosine	CS/CMWNT/GCE	CV	1.6 nM	10nM–2 M	106
L-Tyrosine	Over-oxidized pyrrole- ITO	CV and EIS	1.73 pM (CV), 6.33 pM (EIS)	100 fM–100 mM	104

CPE Carbon Paste Electrode, PGE Pencil Graphite Electrode, GCE Glassy Carbon Electrode, MWCNT Multi-Walled Carbon Nanotube, f-MWCNT functionalized-MWCNT, CMWNT Carboxylated MWCNT, SPCE Screen-Printed Carbon Electrode, AuNP Gold Nanoparticle, PPy Polypyrrole, FeCN Potassium Hexacyanoferrate(II), CS Chitosan, OECT Organic Electrochemical Transistor, ITO Indium Tin Oxide.

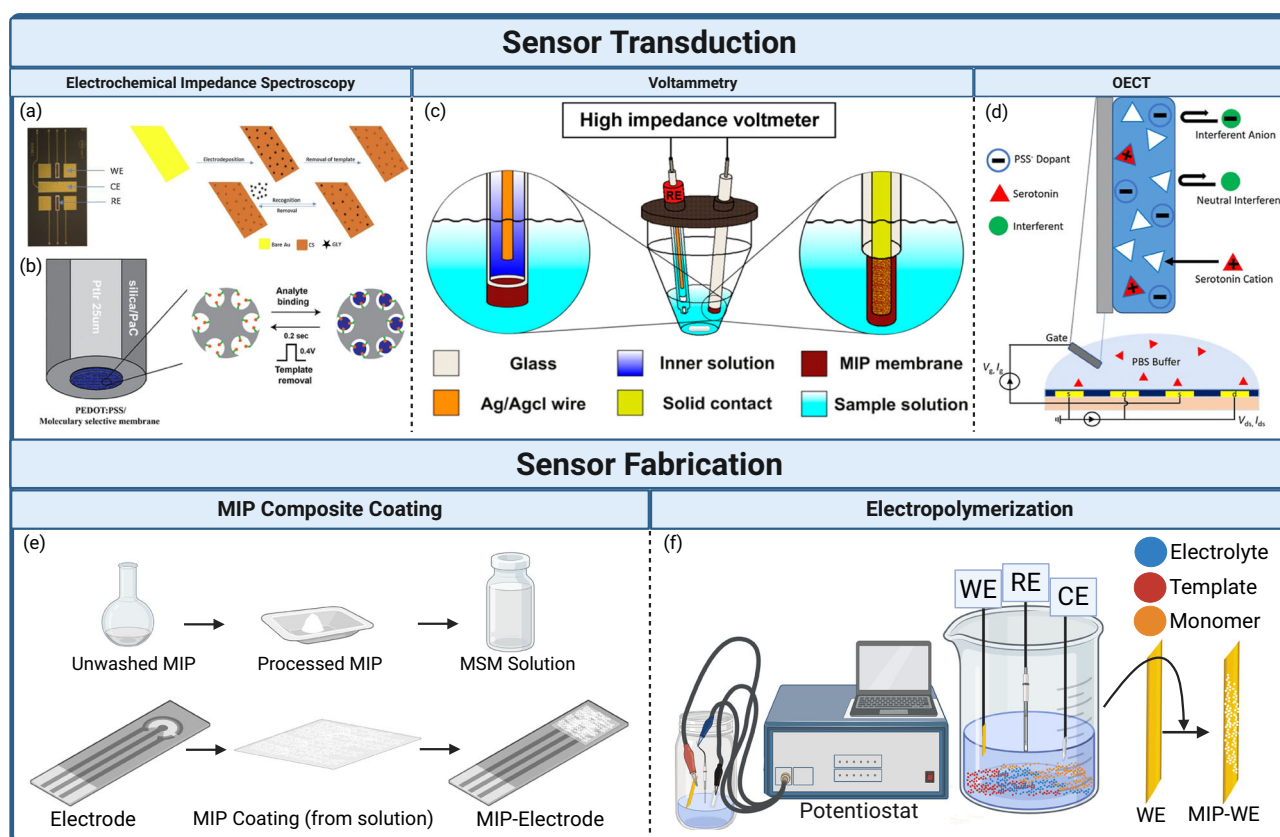


Fig. 5 | General overview of MIP-Based AA sensor Transduction and Fabrication methods. **a** Example of a Glyphosate EIS Sensor¹⁴⁸, **b** Example of an EIS Dopamine Sensor¹⁰⁵, **c** Example of a Voltammetric MIP sensor¹⁴⁹, **d** Example of an OECT¹⁵⁰. **e** Schematic overview of the preparation of a MIP composite, by mixing MIPs into a polymer matrix in solution followed by direct coating on the sensing active layer.

This workflow details the processing of bulk-synthesized MIPs for integration into sensor platforms, **f** Schematic overview of electropolymerization through a three-electrode electrochemical cell to form a cross-linked polymer matrix around the template molecules directly on the WE, resulting in a MIP-modified electrode (MIP-WE).

pulse width, the contribution from the charging current is significantly minimized. This ability to enhance the signal-to-noise ratio makes DPV favorable for the analysis of trace molecules. This is particularly advantageous for MIP sensors designed to operate in complex biological matrices, such as in Aryan et al.'s work on the determination of L-Alanine in urine samples⁹⁴ or Xia et al.'s work on detecting L-Tryptophan in human serum⁹². However, the choice of detection method alone is not the primary determinant of performance. The reported LODs of DPV sensors span an enormous range, from 0.6 μ M for the L-Alanine sensor⁹⁴ compared to ~0.74 pg/mL (~6.11 pM) for the L-Cysteine sensor designed by Hou and colleagues⁹⁹ (a difference of almost five orders of magnitude). This significant disparity provides evidence that the sensor's performance is not significantly affected by simply the method of transduction, but includes the nature of the electrode substrate, the properties of nanomaterial modifiers, and the quality of the MIP film itself in achieving high sensitivity.

Square wave voltammetry (SWV)

Similarly in methodology, SWV, employed in the sensors for L-Aspartic Acid¹¹⁰ and L-Serine¹¹¹, represents a more complex and often faster alternative to DPV. Unlike DPV, SWV samples current at the end of both the forward potential pulse and the subsequent reverse potential pulse within each square-wave cycle, resulting in a voltammogram which plots the difference between the forward and reverse currents against the potential of the underlying staircase¹⁰⁸. SWV also shares the primary advantage of DPV in its discrimination against background charging current. However, SWV offers several distinct advantages in speed, as SWV can be performed at effective scan rates up to 1 V/s or faster, whereas DPV is typically limited to rates of 1–10 mV/s¹¹². Furthermore, for electrochemically reversible or quasi-reversible systems, SWV can offer even greater sensitivity than DPV as the reverse pulse in each cycle can lead to a greater net current response through regenerating the initial reactant at the electrode surface¹¹². As such, the choice to use SWV for the L-Aspartic Acid¹¹⁰ and L-Serine¹¹¹ sensors is reasonable, as in the case of Jaiswal et al.'s L-Serine sensor, which is fabricated using a sophisticated layer-by-layer assembly of dual-imprinted polymers, the rapid analysis time afforded by SWV would be beneficial for practical application and high-throughput testing¹¹¹.

The organic electrochemical transistor (OECT)

Organic Electrochemical Transistors (OECTs) mark a shift from simple signal transduction into active signal amplification. For example, the L-Histidine sensor developed by Zhang, L. et al.¹¹³ represents a significant departure from conventional voltammetric approaches discussed above through its utilization of an OECT to detect and monitor L-Histidine in human urine. OECTs work by applying a small voltage to a gate electrode, which drives ions from an electrolyte into the channel¹¹⁴. Crucially, these ions do not merely accumulate at the dielectric-semiconductor interface, as in a traditional field-effect transistor (FET), but instead penetrate and potentially permeate the entire volume of the OMIEC channel. Thus, this design allows a slight change in the ionic flux at the gate-electrolyte interface to produce a large, amplified change in the electronic current between the source and drain¹¹⁵. This bulk modulation mechanism is the source of the OECT's characteristically high transconductance, often surpassing that of conventional organic FETs and sometimes silicon-based transistors^{114,115}. A schematic overview of an OECT can be seen in Fig. 5c, demonstrating its method of sensing/transduction. The sensor characteristics of an OECT also offer compelling advantages for biocompatibility with further improved flexibility, enabling higher conformability to a biological surface, and operations at low voltages (typically <1 V) in aqueous environments¹¹⁴. Furthermore, the intrinsic signal amplification allows for the detection of minor changes lower than the typical physiological ranges of amino acids in a local ionic environment, demonstrated by the 100 nM LOD for the L-Histidine sensor¹¹³. One drawback with OECTs, however, is that the current output is sensitive to the ionic concentration of the dielectric, which may vary substantially for in-vivo conditions. While conventional two or three-electrode electrochemical techniques have demonstrated continued

success, the OECT platform may offer another direct and scalable path to achieving high-gain, low-power, and potentially wearable or implantable biosensing systems.

Sensor fabrication

The successful translation of synthesized MIPs into functional sensors requires their effective integration with the transducer platform. Two principal strategies dominate this integration: ex-situ immobilization of pre-synthesized particles and in situ polymerization directly on the transducer surface. The ex-situ approach (Fig. 5e) is commonly employed to fabricate MIP composites, a mixture of MIP particles in a polymer matrix (membrane). This method utilizes MIPs synthesized independently through, most commonly, bulk or precipitation polymerization. The resulting polymer must undergo extensive post-processing, including physical homogenization to achieve the desired particle size, followed by washing for template removal and drying, and are subsequently dispersed into a supportive matrix, typically comprising a structural polymer (e.g., PVC, polyurethane) and plasticizers. This resulting MIP composite can then be integrated onto the electrode's surface through various methods, such as dip coating, spin coating, and more. In contrast, in situ polymerization methods form the MIP layer directly on the transducer surface, offering a streamlined fabrication workflow and enhanced interface characteristics. Electro-polymerization (Fig. 5f) is a prominent in situ technique particularly advantageous for electrochemical sensors⁹⁷. In this process, a potentiostat applies a controlled electrical potential, typically using an electrochemical technique like CV, to the working electrode (WE) immersed in a precursor solution containing the functional monomer, template, and supporting electrolyte. The electrochemical initiation drives the polymerization process, resulting in the deposition of a thin, conformal MIP film directly adhered to the electrode surface (MIP-WE), skipping the potentially destructive post-processing step. Overall, both methods stand as important and usable methods for MIP integration into a sensor platform.

Beyond simply sensing, the performance of an MIP sensor in a wearable situation is closely linked to the physical and chemical properties of its substrate. This material must be mechanically compliant, biocompatible, and conform to skin contact, with the Young's modulus of the substrate ideally matching that of human skin (110.1–499.1 kPa) to ensure adhesion and prevent delamination during movement^{6,116,117}. Common materials include polydimethylsiloxane (PDMS), a flexible and biocompatible silicone elastomer which could also be modified for conductivity; polyurethane (PU)-based elastomers, an inexpensive and flexible material capable of being tailored to various applications; and Styrene Ethylene Butylene Styrene (SEBS), for enhanced stretchability and softness¹¹⁸. Recent developments in stretchable sensors have also highlighted the use of elastomers, such as SEBS and PDMS, for enhanced stretchability and softness for in vivo and in situ applications. Pioneering work in this area by Bao and coworkers, such as a comprehensive wearable BodyNet multimodal sensors and stress sensor with cortisol sweat sensing, demonstrates the clear applicability of wearable sensors in health monitoring^{119,120}. Another approach to improving the performance of modern MIP sensors is the integration of nanomaterials for improved sensor transduction¹²¹. These materials serve to amplify the analytical signal by increasing the electrode's effective surface area and enhancing its electrical conductivity while also providing an improved scaffold for MIP immobilization. Carbon-based nanomaterials like CNTs and graphene (typically in the form of laser-induced graphene (LIG)) are frequently used due to their high porosity and high conductance (lower impedance)¹²². LIG is particularly promising for creating low-cost, high-surface-area electrodes due to its ability to be fabricated directly on flexible substrates like polyimide via laser engraving. Metallic nanoparticles, especially gold nanoparticles (AuNPs), are also widely employed to improve conductivity and provide functional sites for polymer growth^{121,122}. More recently, porous crystalline materials like Metal-Organic Frameworks (MOFs) have also been explored for MIP deposition due to their high surface area and tunable pore structures that can enhance the stability of the MIP layer and increase the density of accessible binding sites¹²³.

Sensor integration

Furthermore, as wearable biosensors draw increasingly more attention to sweat as the preferred biofluid for real-time non-invasive health monitoring, there is a necessity for the efficient management of a sweat sample. To address the lower quantities and inconsistency of natural perspiration ($\geq 10 \mu\text{L}$), current literature demonstrates an increasing trend towards the use of skin-adherent microfluidic systems to enhance sensing volume¹²⁴. These devices incorporate networks of micro-scale channels that wick sweat directly from the skin's pores and transport it to a dedicated sensing chamber. Advanced designs integrate active mechanisms, such as electrowetting-on-dielectric (EWOD), or passive, capillary driven flow control elements to deliver small sample volumes for analysis. Paper-based microfluidics have also emerged as a particularly effective and low-cost solution with a simple paper strip acting as a pump to continuously wick sweat through the sensing chamber and into a reservoir^{11,125}. This sophisticated fluid handling is essential for delivering unadulterated samples, a necessary feature that allows for the detection of minute concentration changes that would otherwise be obscured by contamination or evaporation. Iontophoresis is another method that has emerged to combat the challenges of natural perspiration. This technique operates by employing mild, localized electrical current to facilitate the transdermal delivery of pharmacological sudomotor agents, further stimulating eccrine glands to produce sweat independent of thermoregulation or exercise¹²⁶. Therefore, integration of a miniaturized, programmable iontophoresis module into a flexible, skin-interfaced platform stands as a potential step toward mitigating the physiological challenges of natural perspiration and commercialization¹²⁷. However, there are also many challenges for the implementation of iontophoresis, including the mitigation of skin irritation associated with traditional direct current (DC) iontophoresis, though this can be mitigated by employing significantly lower currents and reducing the frequency of iontophoresis^{126,128}. The choice of sudomotor agent has significant implications for system design. While pilocarpine has been traditionally used, its effect is limited to approximately one to two hours while the adoption of slowly metabolized agonists like carbachol can address the issue of iontophoresis frequency and sustain sweat production for over 24 hours from a single dose¹²⁸. Furthermore, the reversibility/reusability of these materials still requires significant research for complete integration. The combination of these technologies, such as consistent sweat induction, microfluidic sample handling, and advanced electrochemical sensing, forms the foundation for the recent major advances in amino acid MIP sweat sensors and the integration into complete platforms.

A representative example demonstrating this integration is the 'NutriTrek' platform developed by Wang et al.⁹. This system utilizes modified laser-induced graphene (LIG) electrodes further functionalized via electropolymerization with specific MIPs designed to selectively detect target amino acids. The detection mechanism, using DPV, relies on the direct electrochemical oxidation of the target analyte (e.g., Tyrosine) after it binds within the MIP cavity (Fig. 6i, k). By fabricating an array of these LIG-MIP sensors, each tailored for a different analyte using MIPs, the NutriTrek platform successfully achieves the simultaneous and continuous detection of all essential amino acids (Fig. 6m). The NutriTrek device architecture (Fig. 6h, j) showcases a comprehensive approach to wearable sweat analysis. It integrates not only electrochemical molecular biosensors but also a temperature sensor for calibration and dedicated electrodes for on-demand sweat stimulation via iontophoresis (using Carbachol gel). This addresses the critical challenge of obtaining sufficient sweat volume independent of physical activity. The functionality of the sensor array is supported by sophisticated, integrated electronics (Fig. 6l), enabling voltage regulation, signal acquisition (via Analog-to-Digital Converters, ADCs), data processing (MCU/CPU), and wireless transmission (Bluetooth). The processed data is relayed to a custom mobile application (Fig. 6n) with the entire system packaged into a compact smartwatch form (Fig. 6o). Wang et al.'s

work serves as a representative hallmark in the field through illustrating the successful integration of MIP-based electrochemical sensing into a holistic wearable platform for health monitoring and demonstrates a clear and vital trend in non-invasive biomarker monitoring.

Overcoming key challenges

The path to clinical and commercial viability is obstructed by several systemic challenges. The most significant challenge for the commercialization of amino-acid MIP sensors is the historically noted high degree of physiological variability in sweat secretion rate composition, both between different individuals (inter-subject) and within the same individual (intra-subject)¹²⁹. These parameters can be influenced by a variety of confounding factors, including ambient temperature, sympathetic nervous system activity, hydration status, diet, and hormonal regulation. However, HPLC analysis by Kuroki and Tsunado posits that the results of intra- and inter-day sweat analyses show relative stability in the concentrations of amino acids regardless of sex¹²⁹. Despite the suggested relative stability of concentrations, there remains a case-by-case difference of amino acid concentration within individuals, evident from the large standard deviation seen across various sweat amino acids. Sweat composition can be influenced by a variety of factors, such as sweat flow rate, reabsorption and secretion mechanisms within the sweat duct, extracellular solute concentrations, hydration, genetic predispositions, and more. While several studies have analyzed and established correlations between amino acid concentrations in sweat and blood, the physiological mechanisms underlying changes in amino acid concentrations are varied and difficult to fully isolate¹³⁰. This inherent variability further complicates the establishment of a reliable correlation between analyte concentrations in sweat and those in blood/plasma, adding doubt to the concrete usage of biomarker sweat sensors as reliable diagnostic devices¹³⁰. To address this, future research must focus on integrated real-time normalization strategies for personalized usage, such as simultaneous monitoring of conductivity or reference electrolytes as proxies for sweat rate, and local skin temperature. Furthermore, more research needs to be conducted on the direct relationship of sweat-AA concentrations as specific disease biomarkers. This correlation between sweat and blood is the linchpin for many envisioned clinical applications that aim to use sweat as a surrogate for blood tests. This issue has been a primary cause of disillusionment in the commercial sector, as the biological basis for their target application proved to be less robust than initially hoped. Furthermore, the commercialization of a wearable sensor ideally provides truly continuous monitoring and reusability. Traditional MIPs often bind to their target with such strength that harsh chemical washing is needed for removal. A recent and important advancement is the development of in situ electrochemical regeneration for an MIP sensor¹⁰⁵. This solution employs an applied electrical potential to generate electrostatic repulsion forces that gently eject the bound analyte from the MIP cavity demonstrated in Wang et al.'s Nutritrek amino acid MIP sensor array and Hemed et al.'s dopamine MIP sensor^{9,105}. This capability enables the long-term, continuous monitoring of biomarkers. MIPs also present an inherent challenge in their synthesis and post-processing, as imprinting small, flexible, and water-soluble amino acid templates often results in a heterogeneous mix of low-affinity binding sites that can be damaged by harsh removal methods⁸⁴. There is also distinct variability noticeable within the synthesis process of the MIPs, capable of resulting in dud batches. Overcoming this trial-and-error nature of MIP development has been a bottleneck for manufacturing. However, recent studies have shown it could potentially be addressed through real-time approaches, such as in Babamiri et al.'s work on controllable MIP electrofabrication through Prussian blue nanoparticles, and computational approaches to optimize polymerization parameters, accelerating development, improving batch-to-batch consistency, and ensuring sensor performance^{131,132}. Still, several on-skin related challenges compromise the quality of the measurement. Sweat is a complex matrix containing high concentrations of electrolytes, metabolites (e.g., lactate, urea), structurally similar amino acids, and varying pH levels. These factors can interfere with the MIP binding mechanism or the electrochemical

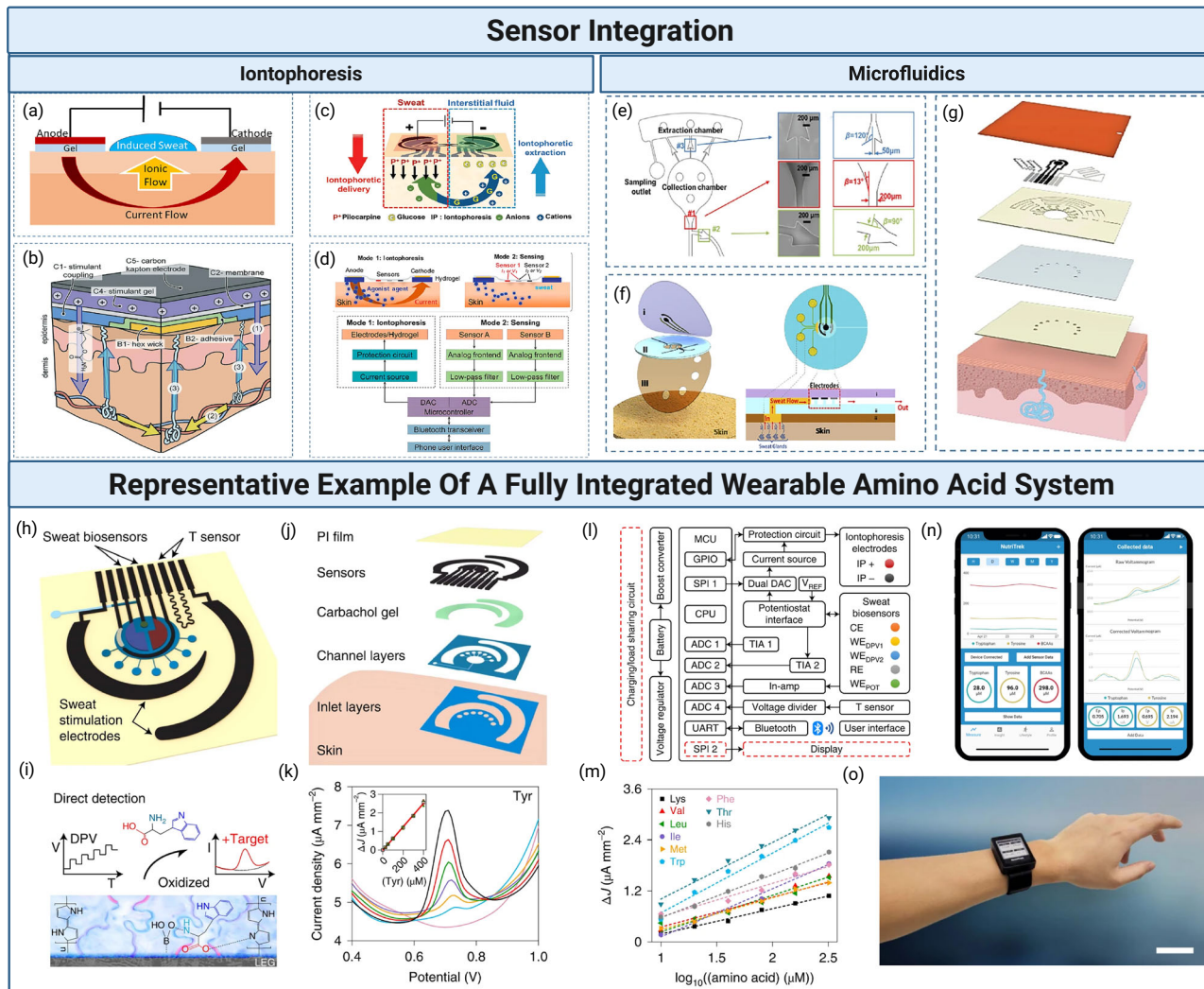


Fig. 6 | Schematic overview of integration methods and integrated systems for wearable sweat sensing, showing key components for sensor integration.
 a Schematic illustrations detailing the sweat induction process through iontophoresis¹, b example of iontophoresis for on-demand sweat induction¹, c illustrated delivery process of iontophoretic sweat induction¹, d schematic overview of iontophoresis integration in a sensing platform¹, e demonstration of skin-mounted microfluidic network¹, f example of microfluidic electrochemical detection

system¹, g schematic overview of a laser-engraved microfluidic platform¹, h schematic depiction of NutriTrek device⁹, i detection mechanism of LIG-MIP sensors⁹, j layer assembly of the NutriTrek device⁹, k DPV voltammograms for Tyrosine exposure on LIG-MIP sensors⁹, l Block electrical diagram of NutriTrek's integrated electronics⁹, m indirect detection of all essential AA's using Wang et al.'s sensors⁹, n Mobile application for point-of-care monitoring via NutriTrek⁹, o NutriTrek full integrated system design/smartwatch⁹.

transduction, for instance, fluctuations in ionic strength can alter the Debye length and impact the performance of EIS or OECT sensors. Furthermore, continuous contact with the skin leads to biofouling from endogenous sources on the skin surface, such as keratinocytes, lipids, and environmental debris, potentially passivating the electrode surface and leading to signal drift and reduced sensitivity over time. Strategies to mitigate this include the development of advanced antifouling coatings, such as zwitterionic polymers or hydrogel membranes and the implementation of continuous calibration techniques¹³³. Furthermore, evaporation can further artificially concentrate analytes, and the mixing of freshly secreted sweat with older accumulated sweat can invalidate measurements, necessitating the creation of tailored fluidic systems to ensure a flow of fresh samples to the sensor.

The future of MIP-based sweat sensing

The most transformative opportunities for the future of this field lie in the intersection between amino acid MIP biosensors and artificial intelligence^{134,135}. This potential relationship would be positioned to amplify the potential of continuous biomarker monitoring to true commercialization. The complex datasets generated by wearable amino-acid sensor arrays

are often too noisy and convoluted for simple interpretation. Machine learning algorithms could act as essential tools for the real-time processing of this data, detecting patterns, filtering out noise, performing personalized calibration, and ultimately providing precise health monitoring^{136,137}. This combination has the potential to redefine how we traditionally view biomarkers^{134–136}. The classical model for biomarkers involves measuring the concentration of a single analyte against a static threshold. However, the sensor-to-AI model enables a move toward identifying complex, multi-analyte signatures (various patterns over time that are far more predictive of a physiological state). For example, an algorithm might learn that a subtle decrease in sweat tryptophan, combined with a specific spike in sweat rate and a stable pH, all occurring within a 30-minute window, is a highly predictive signature of an impending metabolic shift or neurological event. This multi-variate pattern could become the new biomarker, unlocking a level of diagnostic precision unattainable with single-analyte measurements. Figure 7 demonstrates the potential use cases of wearable MIP amino acid sensors commercialized with algorithms for both patient and everyday consumer usage. This could include low-cost, reusable wearable devices for specific point-of-care applications, such as neonatal PKU screening in

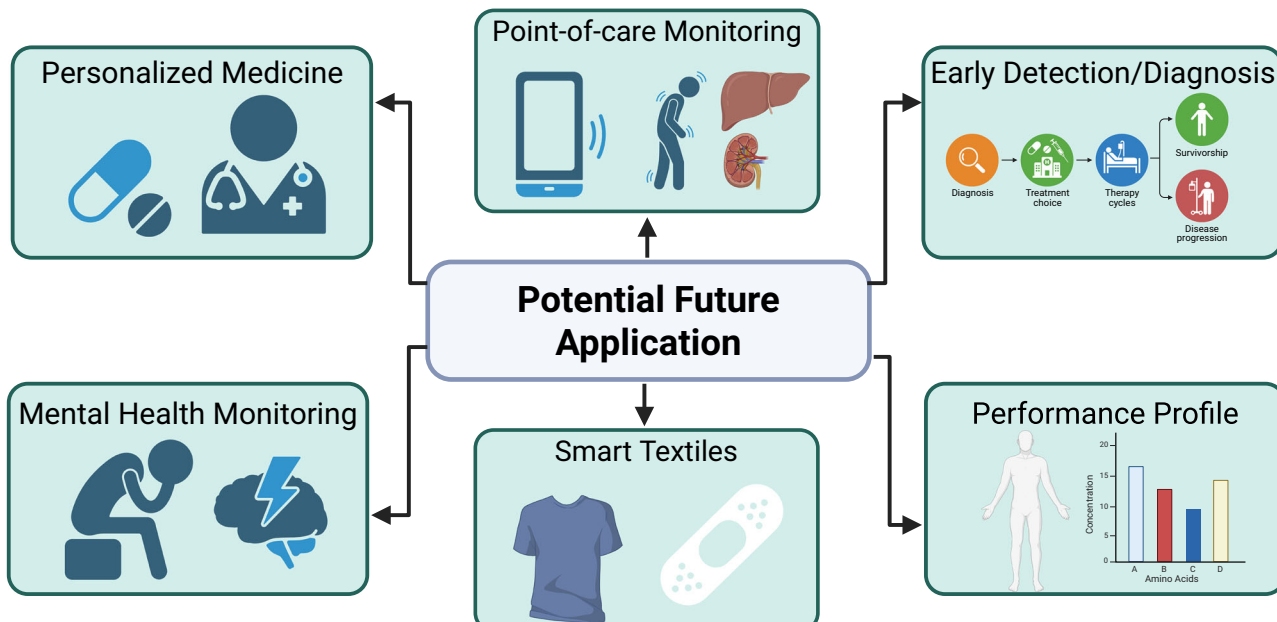


Fig. 7 | Potential future applications of MIP-based sweat sensors, including personalized medicine, point-of-care monitoring, early disease detection, mental health monitoring, smart textiles, and performance profiling.

resource-limited settings, as well as fully integrated continuous monitoring systems for managing chronic diseases, assisting in personalized medicine, implementing into textiles, and managing early risk factors for many health conditions.

Conclusion

MIPs have established themselves in the current literature as a highly promising class of recognition materials for the development of sensitive, selective and potentially wearable biosensors. The combination of their operational robustness, tailored selectivity, cost-effective production efficiency, and high degree of sensitivity makes them compelling candidates for engineering the next generation of wearable biosensors and health monitoring devices. When applied for quantifying amino acids in sweat, MIP-based platforms offer a new modality of non-invasive and continuous analyte detection with the goal of real-time health monitoring. The ability to track fluctuations in an individual's amino acid profile can yield profound and clinically relevant insights into metabolic regulation, organ function, physiological responses, and serve as disease biomarkers, directly advancing the objectives of precision medicine. However, there is still much to be said about the successful transition of this technology from controlled laboratory settings to real-world clinical/consumer applications. Substantial research and development efforts are still required, such as improving in situ sensor regeneration for long-term usage, substantiating causations and correlations with sweat amino acids and health disorders, and establishing multimodal wearable devices, likely powered by artificial intelligence, to account for the individual nature of subject-specific physiological variability. A clear path towards overcoming these obstacles lies within continued innovations across separate fields, ranging from polymer science and microfabrication to wearable electronics and computational data analysis. Rigorous, interdisciplinary investigation is necessary to fully explore and utilize the rich diagnostic potential of sweat. In this pursuit, a future in which healthcare is more proactive, predictive, and personalized, may potentially be on the horizon.

Data availability

No datasets were generated or analyzed during the current study.

Received: 16 August 2025; Accepted: 1 November 2025;
Published online: 09 January 2026

References

1. Gao, F. et al. Wearable and flexible electrochemical sensors for sweat analysis: a review. *Microsyst. Nanoeng.* **9**, 1 (2023).
2. Jia, W. et al. Electrochemical tattoo biosensors for real-time noninvasive lactate monitoring in human perspiration. *Anal. Chem.* **85**, 6553–6560 (2013).
3. Kim, J. et al. Wearable biosensors for healthcare monitoring. *Nat. Biotechnol.* **37**, 389–406 (2019).
4. Bandodkar, A. J., Jeang, W. J., Ghaffari, R. & Rogers, J. A. Wearable sensors for biochemical sweat analysis. *Annu. Rev. Anal. Chem.* **12**, 1–22 (2019).
5. Heikenfeld, J. et al. Accessing analytes in biofluids for peripheral biochemical monitoring. *Nat. Biotechnol.* **37**, 407–419 (2019).
6. Zhao, C., Park, J., Root, S. E. & Bao, Z. Skin-inspired soft bioelectronic materials, devices and systems. *Nat. Rev. Bioeng.* **2**, 671–690 (2024).
7. Min, J. et al. Skin-interfaced wearable sweat sensors for precision medicine. *Chem. Rev.* **123**, 11213–11267 (2023).
8. Wang, B. et al. Wearable aptamer-field-effect transistor sensing system for noninvasive cortisol monitoring. *Sci. Adv.* **8**, eabk0967 (2022).
9. Wang, M. et al. A wearable electrochemical biosensor for the monitoring of metabolites and nutrients. *Nat. Biomed. Eng.* **6**, 1225–1235 (2022).
10. Broza, Y. Y. et al. Disease detection with molecular biomarkers: from chemistry of body fluids to nature-inspired chemical sensors. *Chem. Rev.* **119**, 11761–11817 (2019).
11. Garg, M. et al. Molecularly imprinted wearable sensor with paper microfluidics for real-time sweat biomarker analysis. *ACS Appl. Mater. Interfaces* **16**, 46113–46122 (2024).
12. Khatib, M. & Haick, H. Sensors for volatile organic compounds. *ACS Nano* **16**, 7080–7115 (2022).
13. Antonelli, G. et al. Integrating machine learning and biosensors in microfluidic devices: a review. *Biosens. Bioelectron.* **263**, 116632 (2024).
14. Sempionatto, J. R., Lasalde-Ramírez, J. A., Mahato, K., Wang, J. & Gao, W. Wearable chemical sensors for biomarker discovery in the omics era. *Nat. Rev. Chem.* **6**, 899–915 (2022).

15. Coskun, A., Savas, I. N., Can, O. & Lippi, G. From population-based to personalized laboratory medicine: continuous monitoring of individual laboratory data with wearable biosensors. *Crit. Rev. Clin. Lab. Sci.* **62**, 198–227 (2025).

16. Gao, W. et al. Flexible electronics toward wearable sensing. *Acc. Chem. Res.* **52**, 523–533 (2019).

17. Ibrahim, N. F. A. et al. A comprehensive review of the recent developments in wearable sweat-sensing devices. *Sensors* **22**, 7670 (2022).

18. Ryan, P. J., Riechman, S. E., Fluckey, J. D. & Wu, G. Interorgan metabolism of amino acids in human health and disease. in *Advances in Experimental Medicine and Biology* Vol. 1332 129–149 (Springer, 2021).

19. Miyajima, M. Amino acids: key sources for immunometabolites and immunotransmitters. *Int. Immunol.* **32**, 435–446 (2020).

20. Beaumont, M. & Blachier, F. Amino acids in intestinal physiology and health. in *Advances in Experimental Medicine and Biology* Vol. 1265 1–20 (Springer, 2020).

21. Bucur, B., Purcarea, C., Andreeescu, S. & Vasilescu, A. Addressing the selectivity of enzyme biosensors: solutions and perspectives. *Sensors* **21**, 3038 (2021).

22. Wang, L. & Zhang, W. Molecularly imprinted polymer (MIP) based electrochemical sensors and their recent advances in health applications. *Sens. Actuators Rep.* **5**, 100153 (2023).

23. Lowdon, J. W. et al. MIPs for commercial application in low-cost sensors and assays - An overview of the current status quo. *Sens. Actuators B Chem.* **325**, 128973 (2020).

24. Baker, L. B. & Wolfe, A. S. Physiological mechanisms determining eccrine sweat composition. *Eur. J. Appl. Physiol.* **120**, 719–752 (2020).

25. Chen, Y.-L., Kuan, W.-H. & Liu, C.-L. Comparative study of the composition of sweat from eccrine and apocrine sweat glands during exercise and in heat. *Int. J. Environ. Res. Public Health* **17**, 3377 (2020).

26. Bolliger, M. et al. Mass spectrometry-based analysis of eccrine sweat supports predictive, preventive and personalised medicine in a cohort of breast cancer patients in Austria. *EPMA J.* **16**, 165–182 (2025).

27. Burat, B. et al. Sweat proteomics in cystic fibrosis: discovering companion biomarkers for precision medicine and therapeutic development. *Cells* **11**, 2358 (2022).

28. Lieu, E. L., Nguyen, T., Rhyne, S. & Kim, J. Amino acids in cancer. *Exp. Mol. Med.* **52**, 15–30 (2020).

29. Klaessens, S., Stroobant, V., De Plaen, E. & Van den Eynde, B. Systemic tryptophan homeostasis. *Front. Mol. Biosci.* **9**, 897929 (2022).

30. Martinez-Reyes, I. & Chandel, N. S. Mitochondrial TCA cycle metabolites control physiology and disease. *Nat. Commun.* **11**, 102 (2020).

31. van Spronsen, F. J. et al. Phenylketonuria. *Nat. Rev. Dis. Prim.* **7**, 36 (2021).

32. Chen, T. et al. Newborn screening of maple syrup urine disease and the effect of early diagnosis. *Clin. Chim. Acta* **548**, 117483 (2023).

33. Meyer, F. et al. Molecular mechanism contributing to malnutrition and sarcopenia in patients with liver cirrhosis. *Int. J. Mol. Sci.* **21**, 5357 (2020).

34. Mansoori, S., Ho, M. Y., Ng, K. K. & Cheng, K. K. Branched-chain amino acid metabolism: pathophysiological mechanism and therapeutic intervention in metabolic diseases. *Obes. Rev.* **25**, e13702 (2024).

35. Oyovwi, M. O. & Atere, A. D. Exploring the medicinal significance of L-Arginine mediated nitric oxide in preventing health disorders. *Eur. J. Med. Chem. Rep.* **12**, 100175 (2024).

36. Jakubowski, H. & Witucki, L. Homocysteine metabolites, endothelial dysfunction, and cardiovascular disease. *Int. J. Mol. Sci.* **26**, 746 (2025).

37. Chen, C.-L., Hsu, S.-C., Ann, D. K., Yen, Y. & Kung, H.-J. Arginine signaling and cancer metabolism. *Cancers* **13**, 3541 (2021).

38. Correia, A. S. & Vale, N. Tryptophan metabolism in depression: a narrative review with a focus on serotonin and kynurenone pathways. *Int. J. Mol. Sci.* **23**, 8493 (2022).

39. Gong, X., Chang, R., Zou, J., Tan, S. & Huang, Z. The role and mechanism of tryptophan - kynurenone metabolic pathway in depression. *Rev. Neurosci.* **34**, 313–324 (2023).

40. Smith, K. A., Morris, J. S., Friston, K. J., Cowen, P. J. & Dolan, R. J. Brain mechanisms associated with depressive relapse and associated cognitive impairment following acute tryptophan depletion. *Br. J. Psychiatry* **174**, 525–529 (1999).

41. Hood, S. D. et al. Effects of tryptophan depletion on selective serotonin reuptake inhibitor-remitted patients with obsessive compulsive disorder. *J. Psychopharmacol.* **31**, 1615–1623 (2017).

42. Aquilani, R. et al. Several dementia subtypes and mild cognitive impairment share brain reduction of neurotransmitter precursor amino acids, impaired energy metabolism, and lipid hyperoxidation. *Front. Aging Neurosci.* **15**, 1237469 (2023).

43. Sikonja, J. et al. Clinical and genetic characteristics of two patients with tyrosinemia type 1 in Slovenia - a novel fumarylacetoacetate hydrolase (FAH) intronic disease-causing variant. *Mol. Genet. Metab. Rep.* **30**, 100836 (2022).

44. Gobeil, E. et al. Mendelian randomization analysis identifies blood tyrosine levels as a biomarker of non-alcoholic fatty liver disease. *Metabolites* **12**, 440 (2022).

45. Ma, J. et al. Increased serum phenylalanine/tyrosine ratio associated with the psychiatric symptom of anti-NMDAR encephalitis. *Front. Neurol.* **15**, 1434139 (2024).

46. Ho, C. S. H., Tay, G. W. N., Wee, H. N. & Ching, J. The utility of amino acid metabolites in the diagnosis of major depressive disorder and correlations with depression severity. *Int. J. Mol. Sci.* **24**, 2231 (2023).

47. Hughes, J. H. et al. Dietary restriction of tyrosine and phenylalanine lowers tyrosinemia associated with nitisinone therapy of alkaptonuria. *J. Inherit. Metab. Dis.* **43**, 259–268 (2020).

48. Long, J. et al. Metabolite biomarkers of type 2 diabetes mellitus and pre-diabetes: a systematic review and meta-analysis. *BMC Endocr. Disord.* **20**, 174 (2020).

49. Li, S. et al. The association between leucine and diabetic retinopathy in different genders: a cross-sectional study in Chinese patients with type 2 diabetes. *Front. Endocrinol.* **13**, 806807 (2022).

50. Nakajima, H. et al. Leucine and glutamic acid as a biomarker of sarcopenic risk in Japanese people with type 2 diabetes. *Nutrients* **15**, 2400 (2023).

51. Lee, K. S., Lee, Y. & Lee, S. Alanine to glycine ratio is a novel predictive biomarker for type 2 diabetes mellitus. *Diab. Obes. Metab.* **26**, 980–988 (2024).

52. do Prado, W. L. et al. Preliminary evidence of glycine as a biomarker of cardiovascular disease risk in children with obesity. *Int. J. Obes.* **47**, 1023–1026 (2023).

53. Iamarisio, A. et al. Serum dysregulation of serine and glycine metabolism as predictive biomarker for cognitive decline in frail elderly subjects. *Transl. Psychiatry* **14**, 281 (2024).

54. Leonetti, S., Herzog, R. I., Caprio, S., Santoro, N. & Tricò, D. Glutamate-serine-glycine index: a novel potential biomarker in pediatric non-alcoholic fatty liver disease. *Children* **7**, 270 (2020).

55. Klatt, S. et al. A six-metabolite panel as potential blood-based biomarkers for Parkinson's disease. *npj Parkinsons Dis.* **7**, 94 (2021).

56. Zhai, G. et al. Phenylalanine is a novel marker for radiographic knee osteoarthritis progression: the MOST study. *J. Rheumatol.* **48**, 123–128 (2021).

57. Cheng, C. W. et al. Factors associated with elevated plasma phenylalanine in patients with heart failure. *Amino Acids* **53**, 149–157 (2021).

58. Mohammadi, Z. et al. L-arginine impact on inflammatory and cardiac markers in patients undergoing coronary artery bypass graft: a systematic review and meta-analysis of randomized controlled trials. *BMC Cardiovasc. Disord.* **24**, 641 (2024).

59. Tousoulis, D. et al. Mechanisms of Disease: L-arginine in coronary atherosclerosis—a clinical perspective. *Nat. Rev. Cardiol.* **4**, 274–283 (2007).

60. Förstermann, U. & Munzel, T. Endothelial nitric oxide synthase in vascular disease: from marvel to menace. *Circulation* **113**, 1708–1714 (2006).

61. Fan, M. et al. The association between concentrations of arginine, ornithine, citrulline and major depressive disorder: a meta-analysis. *Front. Psychiatry* **12**, 686973 (2021).

62. Hillsley, A. B. & McLachlan, C. S. Assessment of registered clinical trial designs: comparison of L-arginine and/or L-citrulline interventions for hypertension. *Pharmaceuticals* **17**, 477 (2024).

63. Ratchford, S. M. et al. Improved vascular function and functional capacity following L-citrulline administration in patients with heart failure with preserved ejection fraction: a single-arm, open-label, prospective pilot study. *J. Appl. Physiol.* **134**, 328–338 (2023).

64. Klimontov, V. V., Koroleva, E. A., Khapaev, R. S., Korbut, A. I. & Lykov, A. P. Carotid artery disease in subjects with type 2 diabetes: risk factors and biomarkers. *J. Clin. Med.* **11**, 72 (2022).

65. Holeček, M. Serine metabolism in health and disease and as a conditionally essential amino acid. *Nutrients* **14**, 1987 (2022).

66. Piubelli, L. et al. Serum D-serine levels are altered in early phases of Alzheimer's disease: towards a precocious biomarker. *Transl. Psychiatry* **11**, 77 (2021).

67. Panchal, N. K. & Prince, S. E. The NEK family of serine/threonine kinases as a biomarker for cancer. *Clin. Exp. Med.* **23**, 17–30 (2023).

68. Alesi, S., Ghelani, D., Rassie, K. & Mousa, A. Metabolomic biomarkers in gestational diabetes mellitus: a review of the evidence. *Int. J. Mol. Sci.* **22**, 5512 (2021).

69. Shin, H. E., Park, S. J., Han, Y.-H., Cho, Y. & Won, C. W. Metabolomic profiles to explore biomarkers of severe sarcopenia in older men: a pilot study. *Exp. Gerontol.* **167**, 111924 (2022).

70. Chang, K.-H. et al. Alterations of sphingolipid and phospholipid pathways and ornithine level in the plasma as biomarkers of Parkinson's disease. *Cells* **11**, 395 (2022).

71. Liu, Z. et al. A panel of four plasma amino acids is a promising biomarker for newly diagnosed bladder cancer. *Clin. Nutr.* **43**, 1599–1608 (2024).

72. Ishinoda, Y. et al. A low arginine/ornithine ratio is associated with long-term cardiovascular mortality. *J. Atheroscler. Thromb.* **30**, 1364–1375 (2023).

73. Lee, S. H. et al. Tryptophan-kynurenone ratio as a biomarker of bladder cancer. *BJU Int* **127**, 445–453 (2021).

74. Török, N., Tanaka, M. & Vécsei, L. Searching for peripheral biomarkers in neurodegenerative diseases: the tryptophan-kynurenone metabolic pathway. *Int. J. Mol. Sci.* **21**, 9338 (2020).

75. Harirchi, P., Bastani, K., Sakhaee, K. & Zahedi, P. Molecularly imprinted polymers as artificial antibodies in therapeutic applications. In *Molecularly Imprinted Polymers: Path to Artificial Antibodies* 443–483 (Springer, 2024).

76. Haupt, K., Medina Rangel, P. X. & Bui, B. T. S. Molecularly imprinted polymers: antibody mimics for bioimaging and therapy. *Chem. Rev.* **120**, 9554–9582 (2020).

77. Wackers, G. et al. Towards a catheter-based impedimetric sensor for the assessment of intestinal histamine levels in IBS patients. *Biosens. Bioelectron.* **158**, 112152 (2020).

78. Refaat, D. et al. Strategies for molecular imprinting and the evolution of MIP nanoparticles as plastic antibodies-synthesis and applications. *Int. J. Mol. Sci.* **20**, 6304 (2019).

79. Nikita, N. et al. The basics of large-scale commercial production of monoclonal antibodies. In *Monoclonal Antibodies* 65–88 (Springer, 2024).

80. Patel, A. K. et al. Chapter 3 - Production, purification, and application of microbial enzymes. In *Microbial-Derived Enzymes: Research, Production and Applications* (ed. Brahmachari, G.) 35–60 (Academic Press, 2023).

81. Sande, M. G. et al. Novel biorecognition elements against pathogens in the design of state-of-the-art diagnostics. *Biosensors* **11**, 418 (2021).

82. Wu, L., Li, X., Miao, H., Xu, J. & Pan, G. State of the art in development of molecularly imprinted biosensors. *VIEW* **3**, 20200170 (2021).

83. Ayankojo, A. G. et al. Synthesis techniques in molecular imprinting: from MIP monoliths to MIP films and nanoparticles. In *Molecularly Imprinted Polymers* (ed. Altintas, Z.) (Springer, 2025).

84. Martins, R. O. et al. Greener molecularly imprinted polymers: strategies and applications in separation and mass spectrometry methods. *TrAC Trends Anal. Chem.* **168**, 117285 (2023).

85. Pisarev, O. A. & Polyakova, I. V. Molecularly imprinted polymers based on methacrylic acid and ethyleneglycol dimethacrylate for L-lysine recognition. *React. Funct. Polym.* **130**, 98–110 (2018).

86. Fuchs, Y., Soppera, O. & Haupt, K. Photopolymerization and photostructuring of molecularly imprinted polymers for sensor applications—A review. *Anal. Chim. Acta* **717**, 7–20 (2012).

87. Chen, Q. et al. Molecularly imprinted photonic hydrogel sensor for optical detection of L-histidine. *Microchim. Acta* **185**, 557 (2018).

88. Najafizadeh, P., Ebrahimi, S. A., Panjehshahin, M. R. & Rezayat Sorkhabadi, S. M. Preparation of a selective L-phenylalanine imprinted polymer implicated in patients with phenylketonuria. *Iran. J. Med. Sci.* **39**, 552–558 (2014).

89. Miao, P. et al. Adsorption and recognition property of tyrosine molecularly imprinted polymer prepared via electron beam irradiation. *Polymers* **15**, 4048 (2023).

90. Zhang, R., Gao, R., Gou, Q., Lai, J. & Li, X. Precipitation polymerization: a powerful tool for preparation of uniform polymer particles. *Polymers* **14**, 1851 (2022).

91. Nergiz, M., Zenger, O. & Baydemir Peşint, G. L-proline determination by molecularly imprinted nanoparticles: a potential nanoscale tool for the diagnosis of metabolic disorders. *J. Chromatogr. A* **1730**, 465106 (2024).

92. Xia, Y., Zhao, F. & Zeng, B. A molecularly imprinted copolymer based electrochemical sensor for the highly sensitive detection of L-tryptophan. *Talanta* **206**, 120245 (2020).

93. Ciriminna, R. et al. The sol-gel route to advanced silica-based materials and recent applications. *Chem. Rev.* **113**, 6592–6620 (2013).

94. Aryan, Z., Rajabi, H. R., Khajehsharifi, H. & Sheydaei, O. Highly selective determination of alanine in a urine sample using a modified electrochemical sensor based on silica nanoparticles-imprinted polymer. *J. Iran. Chem. Soc.* **19**, 4139–4148 (2022).

95. Azalina, M. N., Chua, K. L. & Noorhidayah, I. Theoretical and experimental study of valine molecular imprinted polymer using sol-gel process on silica microparticles surface. *IOP Conf. Ser. Mater. Sci. Eng.* **458**, 012012 (2018).

96. Shchipunov, Y. Biomimetic sol-gel chemistry to tailor structure, properties, and functionality of bionanocomposites by biopolymers and cells. *Materials* **17**, 224 (2024).

97. Mwanza, C., Zhang, W.-Z., Kalulu, M. & Ding, S.-N. Advancing green chemistry in environmental monitoring: the role of electropolymerized molecularly imprinted polymer-based electrochemical sensors. *Green. Chem.* **26**, 8494–8522 (2024).

98. Yu, X. Y. et al. Highly sensitive determination of L-glutamic acid in pig serum with an enzyme-free molecularly imprinted polymer on a carbon-nanotube modified electrode. *Anal. Methods* **15**, 5589–5597 (2023).

99. Hou, H. et al. Electrochemical enantioanalysis of D- and L-cysteine with a dual-template molecularly imprinted sensor. *J. Electrochem. Soc.* **169**, 037506 (2022).

100. Nishchaya, K., Rai, V. K. & Bansode, H. Methacrylic acid as a potential monomer for molecular imprinting: a review of recent advances. *Results Mater.* **18**, 100379 (2023).

101. Dewangan, Y., Berdimurodov, E. & Verma, D. K. Amino acids: classification, synthesis methods, reactions, and determination. in *Amino Acids in Nutrition and Health* 3–23 (Elsevier, 2023).

102. Liu, W. et al. Molecularly imprinted polymers on graphene oxide surface for EIS sensing of testosterone. *Biosens. Bioelectron.* **92**, 305–312 (2017).

103. Alam, I. et al. Molecularly imprinted polymer-amyloid fibril-based electrochemical biosensor for ultrasensitive detection of tryptophan. *Biosensors* **12**, 291 (2022).

104. Roy, S. et al. Ultra-sensitive detection of L-tyrosine using molecularly imprinted electrochemical sensor towards diabetic foot ulcer detection. *Electrochim. Commun.* **117**, 106782 (2020).

105. Hemed, N. M., Leal-Ortiz, S., Zhao, E. T. & Melosh, N. A. On-demand, reversible, ultrasensitive polymer membrane based on molecular imprinting polymer. *ACS Nano* **17**, 5632–5643 (2023).

106. Zhang, J. & Li, R. Electrochemical determination of tyrosine and nitrite using CS/CMWNTs/GCE-modified electrode. *Int. J. Electrochem. Sci.* **13**, 3527–3534 (2018).

107. Dinu, A. & Apetrei, C. Development of a novel sensor based on polypyrrole doped with potassium hexacyanoferrate (II) for detection of L-tryptophan in pharmaceuticals. *Inventions* **6**, 56 (2021).

108. Spinola Machado, S. A. & Cincotto, F. H. Electrochemical methods applied for bioanalysis: differential pulse voltammetry and square wave voltammetry. Tools and Trends in Bioanalytical Chemistry 273–282 (Springer, 2021).

109. Lee, D. H. & Lee, W.-Y. Enantioselective electrochemical L-phenylalanine sensor based on molecularly imprinted polymer embedded with redox probes. *Microchem. J.* **209**, 112641 (2025).

110. Prasad, B. B., Jaiswal, S. & Singh, K. Ultra-trace analysis of D- and L-aspartic acid applying one-by-one approach on a dual imprinted electrochemical sensor. *Sens. Actuators B Chem.* **240**, 631–639 (2017).

111. Jaiswal, S. et al. Enantioselective analysis of D- and L-serine on a layer-by-layer imprinted electrochemical sensor. *Biosens. Bioelectron.* **124–125**, 176–183 (2019).

112. Pena-Zacarias, J., Zahid, M. I. & Nurunnabi, M. Electrochemical nanosensor-based emerging point-of-care tools: progress and prospects. *Wiley Interdiscip. Rev. Nanomed. Nanobiotechnol.* **16**, e2002 (2024).

113. Zhang, L. et al. Selective recognition of histidine enantiomers using novel molecularly imprinted organic transistor sensor. *Org. Electron.* **61**, 254–260 (2018).

114. Marks, A., Griggs, S., Gasparini, N. & Moser, M. Organic electrochemical transistors: an emerging technology for biosensing. *Adv. Mater. Interfaces* **9**, 2102039 (2022).

115. Yu, S., Sun, X., Liu, J. & Li, S. OECT - Inspired electrical detection. *Talanta* **275**, 126180 (2024).

116. Liu, S., Rao, Y., Jang, H., Tan, P. & Lu, N. Strategies for body-conformable electronics. *Matter* **5**, 1104–1136 (2022).

117. Mostafavi Yazdi, S. J. & Baqersad, J. Mechanical modeling and characterization of human skin: a review. *J. Biomech.* **130**, 110864 (2022).

118. Wu, H. et al. Materials, devices, and systems of on-skin electrodes for electrophysiological monitoring and human-machine interfaces. *Adv. Sci.* **8**, 2001938 (2021).

119. Khan, Y. et al. On stress: combining human factors and biosignals to inform the placement and design of a skin-like stress sensor. In *Proc. CHI Conference on Human Factors in Computing Systems* 1–13 (ACM, 2024).

120. Niu, S. et al. A wireless body area sensor network based on stretchable passive tags. *Nat. Electron.* **2**, 361–368 (2019).

121. Lahcen, A. A. & Amine, A. Recent advances in electrochemical sensors based on molecularly imprinted polymers and nanomaterials. *Electroanalysis* **31**, 188–201 (2019).

122. Dinc, S., Kara, M., Erol, K. & Altintas, Z. Contribution of smart materials into molecular imprinting: functionalization of MIPs using carbon-based nanomaterials, quantum dots, and nanoparticles. in *Springer Series on Polymer and Composite Materials* 245–277 (Springer, 2024).

123. Hua, Y., Kukkar, D., Brown, R. J. C. & Kim, K. H. Recent advances in the synthesis of and sensing applications for metal-organic framework-molecularly imprinted polymer (MOF-MIP) composites. *Crit. Rev. Environ. Sci. Technol.* **53**, 258–289 (2023).

124. Moonen, E. J. M., Verberne, W., Peissers, E., Heikenfeld, J. & den Toonder, J. M. J. Discretised microfluidics for noninvasive health monitoring using sweat sensing. *Lab. Chip.* **24**, 5304–5317 (2024).

125. Mogera, U. et al. Wearable plasmonic paper-based microfluidics for continuous sweat analysis. *Sci. Adv.* **8**, eabn1736 (2022).

126. Paul, B. et al. Printed iontophoretic-integrated wearable microfluidic sweat-sensing patch for on-demand point-of-care sweat analysis. *Adv. Mater. Technol.* **6**, 2000910 (2021).

127. Childs, A. et al. Diving into sweat: advances, challenges, and future directions in wearable sweat sensing. *ACS Nano* **18**, 11488–11508 (2024).

128. Bolat, G. et al. Wearable soft electrochemical microfluidic device integrated with iontophoresis for sweat biosensing. *Anal. Bioanal. Chem.* **414**, 5411–5421 (2022).

129. Kuroki, H. & Tsunoda, M. Quantification of amino acids in small volumes of human sweat collected from fingertips of healthy subjects at rest. *J. Pharm. Biomed. Anal.* **257**, 116718 (2025).

130. Spano, J. et al. Investigation of effects of collection conditions on amino acid concentrations in sweat and correlations with their circulating levels in plasma. *Sci. Rep.* **15**, 23198 (2025).

131. Babamiri, B., Farrokhnia, M., Mohammadi, M. & Nezhad, A. S. A novel strategy for controllable electrofabrication of molecularly imprinted polymer biosensors utilizing embedded Prussian blue nanoparticles. *Sci. Rep.* **15**, 8859 (2025).

132. Rohani, F. G., Mohadesi, A. & Ansari, M. Computational design and electropolymerization of molecularly imprinted poly(p-aminobenzoic-acid-co-dapsone) using multivariate optimization for tetradifon residue analysis. *ChemistrySelect* **4**, 12236–12244 (2019).

133. Xu, Z. et al. An anti-fouling wearable molecular imprinting sensor based on semi-interpenetrating network hydrogel for the detection of tryptophan in sweat. *Anal. Chim. Acta* **1283**, 341948 (2023).

134. Di Masi, S., Egidio, G. & Malitesta, C. Optimisation of electrochemical sensors based on molecularly imprinted polymers: from OFAT to machine learning. *Anal. Bioanal. Chem.* **416**, 2261–2275 (2024).

135. Cui, F., Yue, Y., Zhang, Y., Zhang, Z. & Zhou, H. S. Advancing Biosensors with Machine Learning. *ACS Sens* **5**, 3346–3364 (2020).

136. Manoharan, S. & Suryabai, X. T. Sensing the future frontiers in biosensors: exploring classifications, principles, and recent advances. *ACS Omega* **9**, 48918–48987 (2024).

137. Goumas, G., Vlachothanasi, E. N., Fradelos, E. C. & Mouliou, D. S. Biosensors, artificial intelligence biosensors, false results and novel future perspectives. *Diagnostics* **15**, 1037 (2025).

138. Mandarano, M. et al. Kynurenone/tryptophan ratio as a potential blood-based biomarker in non-small cell lung cancer. *Int. J. Mol. Sci.* **22**, 4403 (2021).

139. Acet, O. et al. A rational approach for 3D recognition and removal of L-asparagine via molecularly imprinted membranes. *J. Pharm. Biomed. Anal.* **226**, 115250 (2023).

140. Furtado, A. I. et al. Biomolecular fishing: design, green synthesis, and performance of L-leucine-molecularly imprinted polymers. *ACS Omega* **8**, 9179–9186 (2023).
141. Nguy, T. P. et al. Development of an impedimetric sensor for the label-free detection of the amino acid sarcosine with molecularly imprinted polymer receptors. *Sens. Actuators B Chem.* **246**, 461–470 (2017).
142. Gao, W. et al. Fully integrated wearable sensor arrays for multiplexed *in situ* perspiration analysis. *Nature* **529**, 509–514 (2016).
143. Emaminejad, S. et al. Autonomous sweat extraction and analysis applied to cystic fibrosis and glucose monitoring using a fully integrated wearable platform. *Proc. Natl. Acad. Sci. USA* **114**, 4625–4630 (2017).
144. Zheng, W. et al. Electrochemical sensor based on molecularly imprinted polymer/reduced graphene oxide composite for simultaneous determination of uric acid and tyrosine. *J. Electroanal. Chem.* **813**, 75–82 (2018).
145. Wu, Y. et al. Rapid recognition and determination of tryptophan by carbon nanotubes and molecularly imprinted polymer-modified glassy carbon electrode. *Bioelectrochemistry* **131**, 107393 (2020).
146. Zhong, B. et al. Interindividual- and blood-correlated sweat phenylalanine multimodal analytical biochips for tracking exercise metabolism. *Nat. Commun.* **15**, 624 (2024).
147. Cai, J. et al. A single carbon microyarn-based integrated wearable textile sweat sensor built into a hook-and-loop fastener. *Anal. Chem.* **97**, 15771–15779 (2025).
148. Zouaoui, F. et al. Electrochemical impedance spectroscopy determination of glyphosate using a molecularly imprinted chitosan. *Sens. Actuators B Chem.* **309**, 127753 (2020).
149. Leibl, N., Haupt, K., Gonzato, C. & Duma, L. Molecularly imprinted polymers for chemical sensing: a tutorial review. *Chemosensors* **9**, 123 (2021).
150. Mehrehjedy, P., Toris, A., Wang, K. & Gu, Z. Selective and sensitive OECT sensors with doped MIP-modified GCE/MWCNT gate electrodes for real-time detection of serotonin. *ACS Omega* **10**, 4154–4162 (2025).

Acknowledgements

R.G. acknowledges Jonathan Peng, Ian Wu, and Jeffery Tok for helpful discussions and support. This research received no external funding.

Author contributions

R.G. conducted the literature review, wrote the manuscript, and prepared all figures and tables. M.K. and Z.B. edited the manuscript and provided feedback. This research received no external funding.

Competing interests

The authors declare no competing interests.

Competing Interests

The authors declare no conflict of interest.

Additional information

Correspondence and requests for materials should be addressed to Ruotong Gao.

Reprints and permissions information is available at

<http://www.nature.com/reprints>

Publisher's note Springer Nature remains neutral with regard to jurisdictional claims in published maps and institutional affiliations.

Open Access This article is licensed under a Creative Commons Attribution-NonCommercial-NoDerivatives 4.0 International License, which permits any non-commercial use, sharing, distribution and reproduction in any medium or format, as long as you give appropriate credit to the original author(s) and the source, provide a link to the Creative Commons licence, and indicate if you modified the licensed material. You do not have permission under this licence to share adapted material derived from this article or parts of it. The images or other third party material in this article are included in the article's Creative Commons licence, unless indicated otherwise in a credit line to the material. If material is not included in the article's Creative Commons licence and your intended use is not permitted by statutory regulation or exceeds the permitted use, you will need to obtain permission directly from the copyright holder. To view a copy of this licence, visit <http://creativecommons.org/licenses/by-nc-nd/4.0/>.

© The Author(s) 2025